# Phytochemical synthesis and antimicrobial application of gold nanoparticles from extract of *Artemisia annua*.


UNIVERSITY *of the*
WESTERN CAPE

**by**

**Akhona Ntamo**

A thesis submitted in fulfillment of the requirements for the Master's degree in Nanoscience in the Department of Chemistry, University of *the* Western Cape.

Supervisor:

**Professor Wilfred Mabusela**

Co-Supervisor:

**Professor Martin Onani**

February 2023

# Declaration

I declare that "**Phytochemical synthesis and antimicrobial activity of gold nanoparticles from extract of *Artemisia annua***" is my work that it has not been submitted for any degree or examination in any other university and that all the resources I have used or quoted have been indicated and acknowledged by means of complete references.

**Akhona Ntamo** **Date: February 2023**

Signature……

## Dedication

*I dedicate this thesis to my wonderful and loving Ntamo family and also to myself for believing in me and pushing through difficult situations.*

# Acknowledgments

Special thanks to my supervisors: **Prof. Wilfred Mabusela** and **Prof. Martin Onani** for their encouragement and academic support over the past years. I am very sincere and humble about the opportunities I was exposed to. Nothing can explain my words of appreciation for the guidance and mentoring on this project.

We thank **Prof. Maurice Omolo** of the Center for African Medicinal and Nutritional Flora and Fauna (CAMNFF) at Masinde Muliro University of Science and Technology for providing the research plant *Artemisia annua*.

I would like to express my gratitude to **Ms. Caroline Tyhavazimbi** for the guidance and the role played in the antimicrobial activity of this project.

I would also like to thank **Ms. Zimkhitha Nqakala**, **Ms. Siyasanga Booysen**, and **Ms. Tswellang Mgijima** for their guidance, assistance, and mentorship in the lab. The laughter, and words of encouragement we shared made things easier.



My words of thanks are expanded to everyone in the **Organometallics and Nanomaterials research group** and **Nanotechnology Innovation Centre (NIC)** for providing a conducive environment which made this project a success.

Finally, I would love to thank the **DST** for funding this project of the **Nanoscience program**. I would also like to acknowledge the role of the **physics, chemistry,** and **life science** departments for their contribution to characterization analysis.

# Abstract

Metallic nanoparticles synthesized using chemical methods and physical methods are considered toxic to the environment due to the use of toxic solvents. The biological synthesis methods such as the use of plant extracts are of interest because they are biocompatible, environmentally friendly, and relatively cost-effective. Gold nanoparticles (AuNPs) have been synthesized using plant aqueous extract as a reducing agent and have shown selective antibacterial activity and good antifungal properties. This study used an aqueous extract of *Artemisia annua* to synthesize biogenic AuNPs and tested them for antimicrobial activity. The *A.annua*-AuNPs were characterized using Ultraviolet-visible spectroscopy (UV-Vis), Fourier transform infrared spectroscopy (FTIR), Dynamic light scattering (DLS), and High-resolution transmission electron microscopy (HRTEM). The UV-Vis spectrum of the *A.annua*-AuNPs showed a surface plasmon resonance (SPR) peak ~550 nm wavelength. The FTIR analysis revealed that –OH groups were present on both plant extract and AuNPs. The DLS showed a Zeta potential of -38.2 ± 1.77 and hydrodynamic radius of 107.94 ± 5.73, PDI of 0.479 ± 0.0174. These results show that the synthesized AuNPs were polydispersed and stable. The HRTEM studies showed that the average particle size of the synthesized AuNPs was ~50 nm and the majority of particles are quasi-spherical with larger triangles and truncated triangular-shaped particles. The EDX spectroscopy analysis of the AuNPs confirmed the presence of gold ions in the samples through strong optical adsorption peaks observed around 2.5, 9.7, and 11.4 KeV.

The stability testing of *A.annua*-AuNPs on biological media (LB-broth and MHB) showed stability at 25 ºC. The antimicrobial studies of the synthesized gold nanoparticles were investigated against the Gram-positive bacteria named *Staphylococcus aureus* (ATCC 25923), *Staphylococcus epidermidis* (ATCC 12228), and *Methicillin-resistant Staphylococcus aureus* MRSA (ATCC 33591) together with Gram-negative bacteria named *Klebsiella pneumoniae* (ATCC 13883), *Escherichia coli* (ATCC 35281), and *Pseudomonas aeruginosa* (ATCC 27853) using agar well diffusion method. *Artemisia annua* water extract showed positive antibacterial activity against *S. epidermidis*, MRSA, and *K. pneumoniae. A.annua*-AuNPs showed high activity against *K. pnuemoniae* and *E.coli*, both with MIC value of 137 µg/ml, and the lowest activity on MRSA, with a MIC value of 550 µg/ml.

**Keywords**

Gold nanoparticles (AuNPs)

*Artemisia annua*

Phytochemical synthesis

Antimicrobial activity

# Table of Contents

# List of figures

# List of tables

## List of abbreviations

| | |
|---|---|
| *A.annua* | - Artemisia annua |
| *A.annua*-AuNPs | - Artemisia annua-mediated gold nanoparticles |
| AMR | - antimicrobial resistance |
| ASDs | - Autism spectrum disorders |
| AuNPs | - Gold nanoparticles |
| CDC | - Centres for Disease Control and Prevention |
| CNTs | - Carbon nano tubes |
| DLS | - Dynamic light scattering |
| DST | - Department of Science and Technology |
| DTH | - Delayed-type hypersensitivity |
| *E.coli* | - *Escherichia coli* |
| EDX | - Energy Dispersive X-ray |
| FTIR | - Fourier transform infrared spectroscopy |
| $HAuCl_4 \bullet XH_2O$ | - Gold Chloride Hydrate |
| HRTEM | - High-resolution transmission electron microscopy |
| JCPDS | - Joint Committee on Powder Diffraction Standards |
| *K.pneumoniae* | - *Klebsiella pneumoniae* |
| LB-broth | - Lysogeny broth |
| MHB | - Mycorrhiza helper bacteria |
| MIC | - Minimum inhibitory concentration |
| MRSA | - Methicillin-resistant Staphylococcus aureus |
| NIC | - Nanotechnology Innovation Centre |
| nM | - Nanometres |

| | |
|---|---|
| NPs | - Nanoparticles |
| *P.aeruginosa* | - *Pseudomonas aeruginosa* |
| PDI | - Polydispersity index |
| *S.aureus* | - *Staphylococcus aureus* |
| *S.epidermidis* | - *Staphylococcus epidermidis* |
| SAED | - Selected electron diffraction |
| SDG | - Sustainable development goals |
| SPR | - Surface plasmon resonance |
| U.S | - United States |
| UV-Vis | - Ultraviolet-visible spectroscopy |
| VRSA | - Vancomycin-resistant S. aureus |
| WHO | - World Health Organisation |
| XRD | - X-ray powder diffraction |
| $\lambda_{max}$ | - Maximum absorption |

## Thesis outline

This thesis is divided into 4 chapters that are described below.

### Chapter 1

This chapter introduces the scope of the study. It gives a brief introduction to microorganism infections and antimicrobial-resistant microorganisms. This chapter also represents a literature review of the field of nanotechnology, nanomaterials, their applications, and their synthesis procedure. The phytochemical synthesis is discussed with the proposed mechanism. The plant species *Artemisia annua* is also reported with background information on literature related to its antimicrobial activity. It narrows the focus to the application of AuNPs in the biomedical field as an antimicrobial agent for infections which is discussed intensively. It expands into general information about gold nanoparticles and *Artemisia annua* plant species. This chapter ends with the hypothesis, aims, and objectives of this project.

### Chapter 2

This chapter starts with the materials and methods used for the phytochemical synthesis of AuNPs from *Artemisia annua* plant extract. Detail about chemical purity as well as the analytical instruments and the suppliers is provided in this chapter. This is followed by the optimization procedure where the reaction conditions were changed and monitored by UV-VIS spectroscopy. Further characterization methods used on optimized *A.annua*-AuNPs are also outlined in this chapter. The chapter also included the antimicrobial study of the optimized AuNPs which were tested for anti-bacterial effects using the agar well diffusion method.



### Chapter 3

This chapter has results and a discussion of the optimization procedure using UV-VIS spectroscopy. The results of the optimized AuNPs are also discussed on techniques such as FTIR, DLS, and HRTEM. The result of antimicrobial activity against 6 bacterial strains is also discussed in this chapter.

**Chapter 4**

This chapter summarized the findings obtained from the synthesis, characterization, and biological applications of *A.annua*-AuNPs. It also links the specific aims and objectives to the outcomes of the study. Furthermore, recommendations and future works are briefly discussed.

# Chapter 1: Literature review

## 1. Introduction

Since ancient times, traditional medicines obtained from plant essential oils and aqueous extracts were used to treat microbial infections; an example is the use of lemon balm (*Melissa officinalis*), garlic (Allium sativum), and tea tree (*Melaleuca alternifolia*) (Suschke et al., 2007; Edwards et al., 2015). Currently, antibiotics are very useful drugs to fight against microbial infections. However, the outbreak of antimicrobial resistance (AMR), jointly with the shortage of newly developed antimicrobial drugs, brings a great threat to the health of both humans and animals (Cheng et al., 2016). The misuse and overuse of antimicrobials have been declared to be the main causes of drug-resistant pathogens (Karakonstantis et al., 2019). The World Health Organisation (WHO) has declared that AMR is one of the top 10 global public health threats faced by humans in 2019 (WHO., 2021). The lack of clean water and sanitation and inadequate prevention and control promotes the spread of microbes, some of which can be resistant to antimicrobial treatments (Parsonage et al., 2017). The cost of AMR to the economy is significant. According to the Centres for Disease Control and Prevention (CDC), antimicrobial resistance adds a 20-billion-dollar surplus in direct healthcare costs in the United States (US) annually (Dadgostar., 2019). Because of superinfections, multiple infections, and reinfections, people spend more time in the hospitals (Eagye et al., 2009) which results in prolonged illness and several health complications (e.g., eczema, multiple sclerosis, etc), disability, and even death (Cassini et al., 2019).



The therapy using antimicrobial drug combinations is another conventional method that is selectively effective for the prevention of bacterial resistance but the main drawback of this medication is cost (Aslam et al., 2015). The quality of life of the patient is also impacted by bacterial infections. An example, Bacterial meningitis caused by *Neisseria meningitidis* can lead to brain damage, paralysis, or stroke (Ahmed et al., 2020). Furthermore, plant-based pathogenic microbes hinder the yield and quality of food production. Plant diseases have caused an increase in food costs due to crop destruction (Osonga et al., 2020). Although plant-based infections exist, the phytochemicals produced by the metabolic pathways of the plant itself result in the suppression of fungi, bacteria, and plant virus infections. These phytochemicals are naturally synthesized by plants to defend themselves against pathogens and predators (Lattanzio et al., 2009). The properties of phytochemicals have resulted in the

increased use of phytochemicals as home remedies and supplements by humans. According to the WHO, 80% of the world's population uses traditional herbal remedies, and 1 in 5 persons in the U.S. frequently consumes herbal products because they are recognized as standard healthcare dietary supplements (Chan et al., 2010).

*Artemisia annua* is a medicinal herb that is well known to contain artemisinin as an active compound (Efferth., 2017). It has been used for antibacterial and anti-inflammatory properties but the spread of artemisinin resistance in *Plasmodium falciparum* malaria has left many, especially in underdeveloped countries vulnerable to malaria-based infections (Ashley et al., 2014). Because of these limitations and disadvantages of the current conventional methods, there is a greater need for the development of a new drug with highly efficient antimicrobial activity, affordable, and available in bulk.

The increasing modern application of nanotechnology in therapeutic uses could be a solution to the discovery of this drug having an enhanced antimicrobial property (Krol et al., 2013). Metallic nanoparticles such as gold nanoparticles (AuNPs) showed promising antibacterial activity against gram-negative bacteria such as *Klebsiella pneumoniae* (Rao et al., 2017) and gram-positive bacteria such as *Staphylococcus aureus* (Suganya et al., 2015). On the other hand, AuNPs synthesized using plant extracts have been previously reported to have antifungal properties and selective antibacterial activity (Zhang et al., 2015). Although the literature shows the importance of AuNPs as an antimicrobial agent, there is a great concern about their toxicity because some contain complexes. In many cases, the toxicity does not come from the AuNPs, but rather from either the non-biocompatible surface ligands (Ali et al., 2019).

The green synthesis method is more favorable than other biological processes for nanoparticle synthesis because it does not require the maintenance of cell cultures and is suitable for large-scale nanoparticle synthesis (Roy and Das., 2015). Further interest in the use of the *A.annua* plant extract in this project is due to the report where stable AuNPs were produced having functionalized groups from phytochemicals without the use of toxic solvents (Basavegowda et al., 2014). Shakibaie and colleagues have reported the synthesis of AuNPs using a green synthesis method. They successfully synthesized AuNPs by using *Tetraselmis suecica* aqueous extract as a reducing agent of chloroauric acid ($HAuCl_4$) solution. They have done this synthesis to investigate whether the *Tetraselmis suecica* will be able to reduce $HAuCl_4$ claiming it is the first report of using this marine microalga. The characterization was carried out and the UV-Vis showed a surface plasmon resonance (SPR) at 530 nm and HRTEM

showed that the AuNPs were all spherical. The leaf extract of *Cassia auriculata* was used to synthesize AuNPs and tested for antidiabetic activity (Kumar et al., 2011). The $HAuCl_4$ solution was reduced at 28 °C for 10 minutes and the AuNPs produced had an average size of 15–25 nm. They concluded that the AuNPs stabilizing and reducing molecules promoted the anti-hyperglycemic effect. Furthermore, the method of green synthesis was used by using grape waste (seed, skin, and stalk) to reduce $HAuCl_4$. The synthesis was done at room temperature for 5 minutes and the AuNPs had an average size of 20–25 nm with a spherical shape dominating (Krishnaswamy et al., 2014). These results show a possibility of the production of AuNPs using plant extracts which aligns with the aim of this project.

### 1.1. Types of microbes and microbial infections

Microbes, often known as microorganisms, are living organisms that are found all around us and are too small to be seen by the human eye (Allen et al., 2015). They are found almost everywhere including the human body, and also exist in many different shapes, such as rods, spheres, and even corkscrews. (Yulo and Hendrickson., 2019). Some are adaptable to extremes like extremely hot or cold temperatures, others to high pressure, and a few, like *Deinococffcus radiodurans*, are resistant to high ionization radiation conditions (Li et al., 2021). Microbes play a significant role in human culture and health in a variety of ways, such as by treating sewage (Okeke et al., 2021), fermenting food (Sharma et al., 2020) as well as producing enzymes, fuel, and other bioactive chemicals (Kumar et al., 2018). Pathogens are the type of microbes that are responsible for causing a broad range of infectious diseases and the most common types include bacteria, viruses, and fungi (Khamesipour et al., 2018). Bacterial infections refer to any disease or condition caused by bacterial growth or toxins (Abubakar et al., 2007). Bacterial infections can be treated with antibiotics which can kill the bacteria or at least stop them from multiplying. The most clinically antibiotic-resistant bacterial organisms reported in the literature are *Enterobacteriaceae*, *Enterobacteriaceae*, *Staphylococcus aureus*, and *Salmonella* species (Schwartz and Morris., 2018). Serious bacterial diseases include tuberculosis, cholera, diphtheria, bacterial meningitis, tetanus, Lyme disease, gonorrhea, and syphilis (Doron and Gorbach., 2008). Diseases caused by fungi are called mycoses and common examples include athlete's foot or fungal infections of the nails (Havlickova et al., 2008). Fungal infections can also cause inflammations of the lungs, or mucous membranes in the mouth or on the reproductive organs, and become life-threatening for people who have a weakened immune system (Li et al., 2019).

Infections caused by viruses are the main causes of disease outbreaks resulting in global pandemics (Holmes et al., 2018). These biological entities can only thrive and multiply in a host, the example is the influenza A virus which has caused a pandemic due to the virus-host interaction between animal hosts and human hosts (Long et al., 2019). Presently, an example of a severe virus is the acute respiratory syndrome coronavirus 2 (SARS-CoV-2) which causes the disease COVID-19 (Pal et al., 2020).

### 1.2. Factors resulting in antimicrobial drug resistance (AMR)

The body's immune system has developed a variety of defenses to limit microbial infections and control inflammatory reactions (Mogensen., 2009). A weakened immune system leaves the body vulnerable to infections and diseases (Honce and Schultz-Cherry., 2019). Factors causing a weakened immune system include aging (Fuentes et al., 2017), obesity and poor diet (Manca et al., 2022), and other underlying health complications such as autism spectrum disorders (ASDs) (Pangrazzi et al., 2020). The ethical approach of the patient also results in AMR. This occurs when a patient has poor compliance with the use of time-dependent antibiotics with a long shelf-life leading to microbial resistance (Parsonage et al., 2017). Missing the scheduled doses and taking the incorrect amount of doses also result in microbial infection not being effectively cured which results in AMR (Singer et al., 2016). Some antimicrobial drugs do not kill all the microbes, which results in some microbes surviving for longer and therefore developing resistance (Levy and Marshall, 2004). The availability of antimicrobials over the counter and without prescription in most developing countries leads to the misuse of these drugs (Byarugaba., 2004). Moreover, poverty was highlighted as the contribution to antimicrobial misuse as some patients could not afford a prescribed medication from the medical practitioner which may cause the development of infection resistance (Okeke et al., 2005). Furthermore, the situation becomes even worse when patients seek treatments from traditional healers using herbal mixtures of unknown compositions. These mixtures may enhance the pathogen survival strategies and contribute to the development of resistance (Fluit et al., 2009). On the other hand, even developed countries encounter an AMR problem through individuals that stop taking doses when their symptoms begin to subside (Hart and Kariuki., 1998).

### 1.3. Current management of antimicrobial resistance and their drawbacks

Pharmaceutical companies play a major role in the research and development of drugs possessing antimicrobial properties. These companies produce hygiene and sanitation products as well as vaccines. However, the pharmaceutical industry was reported to focus more on investing in the development of drugs for chronic diseases and those to improve lifestyle (e.g., Viagra) (Ayukekbong et al., 2017). This results in the long-term solution being the development of control strategies to prevent the emergence of resistance.

#### 1.3.1. Antimicrobial resistance control strategies

Although the human immune system could provide a natural antimicrobial activity, there are antimicrobial drugs that are developed to boost the response. Indigenous communities used traditional medicines and natural products from lemon balm (*Melissa officinalis*), garlic (Allium sativum), and tea tree (*Melaleuca alternifolia*) to fight the infections (Suschke et al., 2007; Edwards et al., 2015). Currently, topical and systemic antimicrobial agents are among the developed drugs to fight microbial infections. Due to the increase in antimicrobial resistance, therapy of antimicrobial combinations was then used to take advantage of different mechanisms of action and synergistic effects (Manohar et al., 2022). Olliaro and Taylor have reported the use of the *Artemisinin* combination treatment against resistant *falciparum* malaria. They reported the major drawback of this treatment to be the success of the cure rate which depends mainly on the level of resistance of the standard drug (Olliaro and Taylor., 2004).



#### 1.3.2. Drawbacks of antimicrobial control strategies

Due to the ease and abundant availability of herbal plants, natural medicines have been developed and utilized for ages for the treatment of infections. However, the therapy using natural products was reported to be associated with an incorrect diagnosis, improper dosage, low hygiene standards, and the secrecy of some healing methods which leaves individuals vulnerable to complicated infections (Fokunang et al., 2011). It is also reported that the use of antibiotics as the current effective accessible drug against infections shows a higher probability of bacterial resistance development because of overuse and misuse (Cancio., 2021; Punjataewakupt et al., 2019). The major drawback of the combination therapy it is associated

with increased costs and further antimicrobial resistance due to the microbe's genetic evolution over time (Aslam et al., 2015; Bottery et al., 2021). In recent years, AuNPs synthesized using plant extracts have been reported as promising antimicrobial agents because of their antibacterial and antifungal properties (Akintelu et al., 2020).

### 1.4. Antimicrobial potential of herbal medicine from *Artemisia annua.*

*Artemisia annua L.* is a herbal plant that is indigenous to temperate Asia but has been naturalized around the world (Zeb et al., 2018). It is commonly known as sweet wormwood, sagewort, and Qinghao (Bilia et al., 2014). *A.annua* belongs to the *Asteraceae* family with over 500 species found throughout all continents except for Antarctica. From sea level to elevated altitudes, the genus *Artemisia L.* adapts to any habitat (Klayman., 1993). The majority of *Artemisia* species were found to grow well in the Northern Hemisphere and at a slightly lower extent in the Southern Hemisphere (Willcox., 2009; Tu ., 2011). The wild of Asia (mainly China, Japan, and Korea) is claimed to be a major source of the *A. annua* plant however it was also introduced in Poland, France, Romania, and the United States, where it became domesticated (Feng et al., 2020). This genus includes perennial, biennial, and annual grasses, shrubs, and bushes with straight or ascending stems that are generally scented. These plants have alternate leaves that are often split, rarely complete, and have smooth edges (Klayman., 1993).



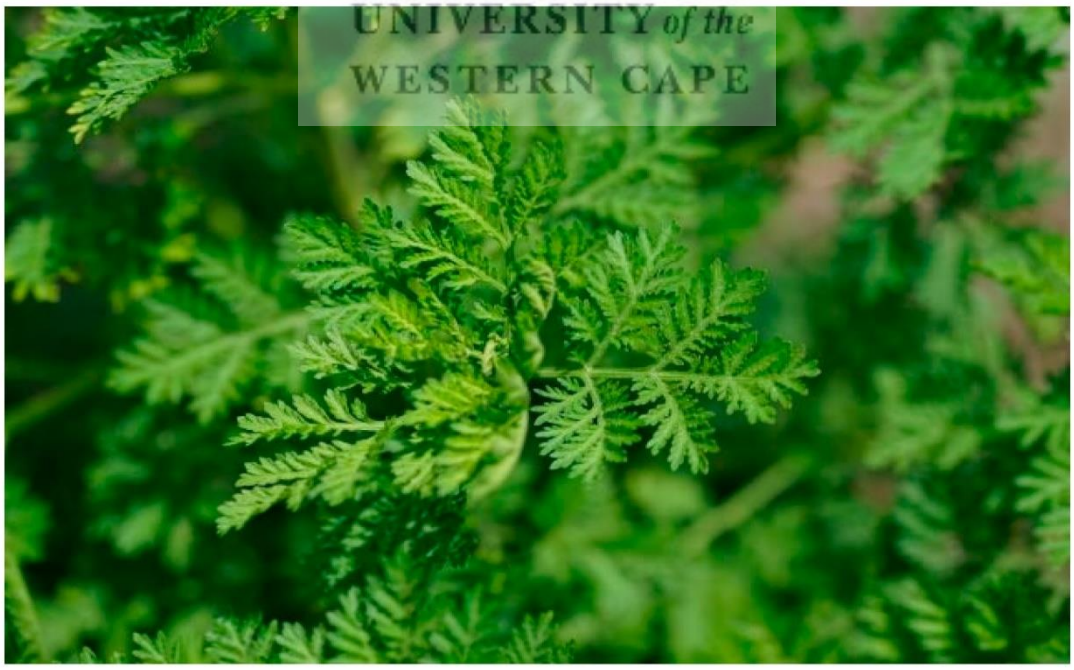

Figure 1.1: The *Artemisia annua* plant (Septembre-Malaterre et al., 2020).

Aweeka and German have reported the *A.annua* plant to be the main natural source for the production of artemisinin and its derivatives, such as dihydroartemisinin, artesunate, artemether, and arteether (Figure 1.2). They also reported the use of these compounds to make combination treatments for the treatment of malaria (Aweeka and German., 2008). Artemisinin-based combination therapy (ACT) is made effective by combining the artemisinin-based compounds with a drug from different classes. An example of standard drugs used includes lumefantrine, mefloquine, amodiaquine, sulfadoxine/pyrimethamine, piperaquine, and chlorproguanil/dapsone (Nosten et al., 2007).

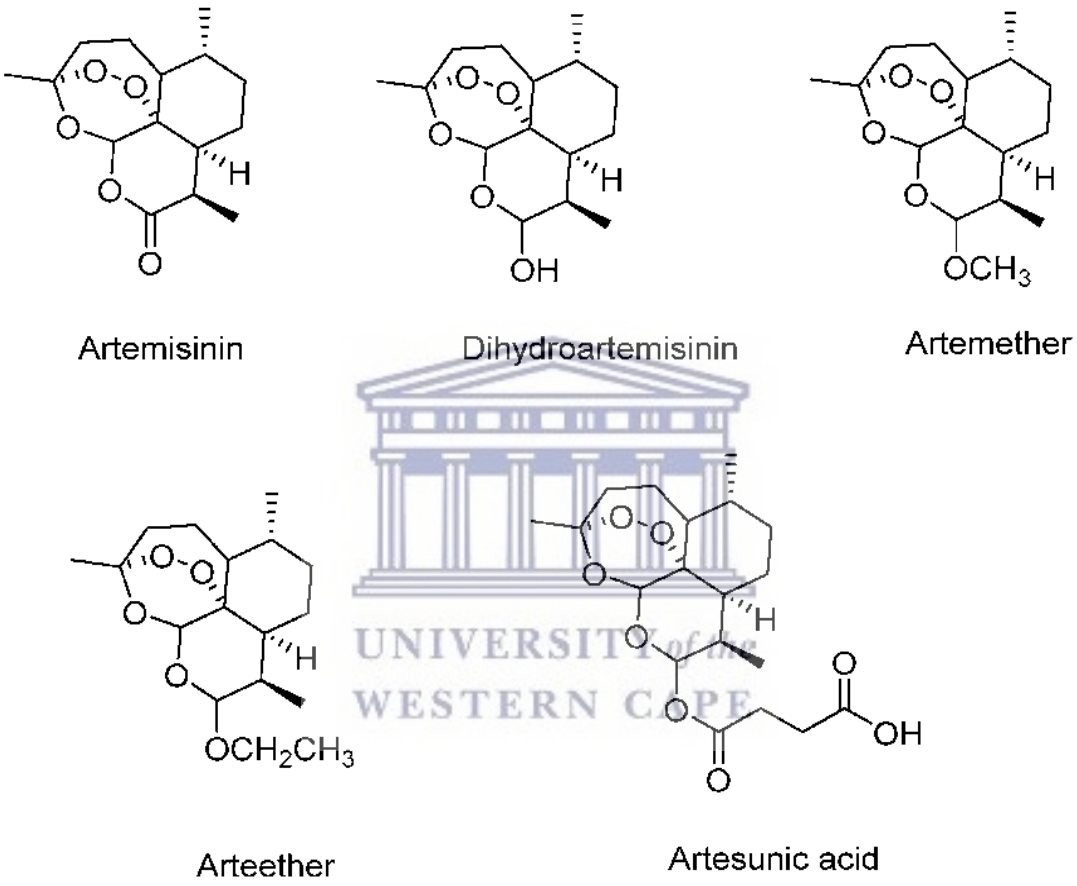


Figure 1.2: Structures of artemisinin and its semi-synthetic derivatives (Jana et al., 2017).

Since prehistoric days, Chinese herbalists have utilized *Artemisia annua* to treat a variety of diseases. In China, Europe, and Africa, the *A. annua* species have been used to treat fever and malaria (Nigam et al., 2019). Furthermore, a national malaria research effort was launched in 1967 where a Chinese scholar, tested over 380 herbal extracts for anti-malarial activity. The species of interest *A. annua* was found as being the most active plant (Khalid et al., 2019). *Artemisia annua* is reported to have anti-hyperlipidemic, anti-plasmodial, anti-convulsant, anti-

inflammatory, anti-microbial, anti-cholesterolemic, and antiviral properties (Singh et al., 2021). It was also reported to also have therapeutic properties such as anti-inflammatory, antitumor, and anti-obesity activities (Septembre-Malaterre et al., 2020). Recently, research done by Nair and colleagues (2022) has reported that the hot-water extracts of *A. annua* are active against SARS-CoV-2 and its variants alpha, beta, gamma, delta, and kappa (Nair et al., 2022). Furthermore, *A.annua* was also reported to be involved in the synthesis of the nanoparticles such as AuNPs using the biosynthesis method and were investigated for their antibacterial activities (Basavegowda et al., 2014). Currently, the field of nanotechnology is growing rapidly owing to the benefits of using plant extracts to synthesize nanomaterials.

### 1.5. Introduction to Nanotechnology and Nanomaterials

Nanotechnology is the emerging science, manufacturing, and application of objects with the smallest dimensions ranging from 1 to 100 nanometres (Hyeon et al., 2015). The term nanotechnology was first proposed by the 1925 Nobel Prize laureate in chemistry called Richard Zsigmondy. He used the term "nanometer" for characterizing the particle size of particles such as gold colloids using a microscope (Zsigmondy., 1909). Richard Feynman, the 1965 Nobel Prize laureate in physics further developed the concept resulting in modern nanotechnology by delivering a lecture at the American Physical Society meeting at Caltech in 1959 introducing the manipulation of matter at the atomic level (Feynman., 1960). Nanotechnology develops methods that are used to synthesize nanomaterials for modern applications. The nanomaterials are applied in fields like drug delivery (Prow et al., 2011), water treatment (Dankovich and Gray., 2011), the food industry (Chaudhry and Castle., 2011), biosensing and others (Basavegowda et al., 2014). In the market, nanotechnology products are found and used to eliminate previous problems of the products used prior. Shapira and Wang have reported on the commercialization of nanotechnology products in China making examples of 5 firms. They reported the firm that produces a fuel additive to reduce toxic emissions and improve vehicle fuel consumption. The company for air cleaning also reported where nanofillers were used in the manufactured products. Ultrafine precipitated calcium carbonates used in building materials were also one of the currently commercialized nanotechnology products that were reported. Furthermore, other commercial products were antibacterial materials and fibers containing silver nanoparticles to enhance the antibacterial properties of silver (Shapira and Wang., 2009).

### 1.5.1. Classification of nanomaterials

Nanomaterials are materials with a high surface area to volume ratio resulting in different physicochemical characteristics from those of the bulk material, and this relies on their size and shape (Saleh., 2020). Surprisingly, by modifying their shape and size at the nanoscale level, nanomaterials exhibit distinct characteristics with new features and capabilities (Qiu et al., 2020). Nanomaterials exist in a variety of morphologies, such as nanorods, nanoparticles, and nanosheets (Sannino., 2021). Classifications of nanomaterials according to their dimensionality are shown in Figure 1.3.

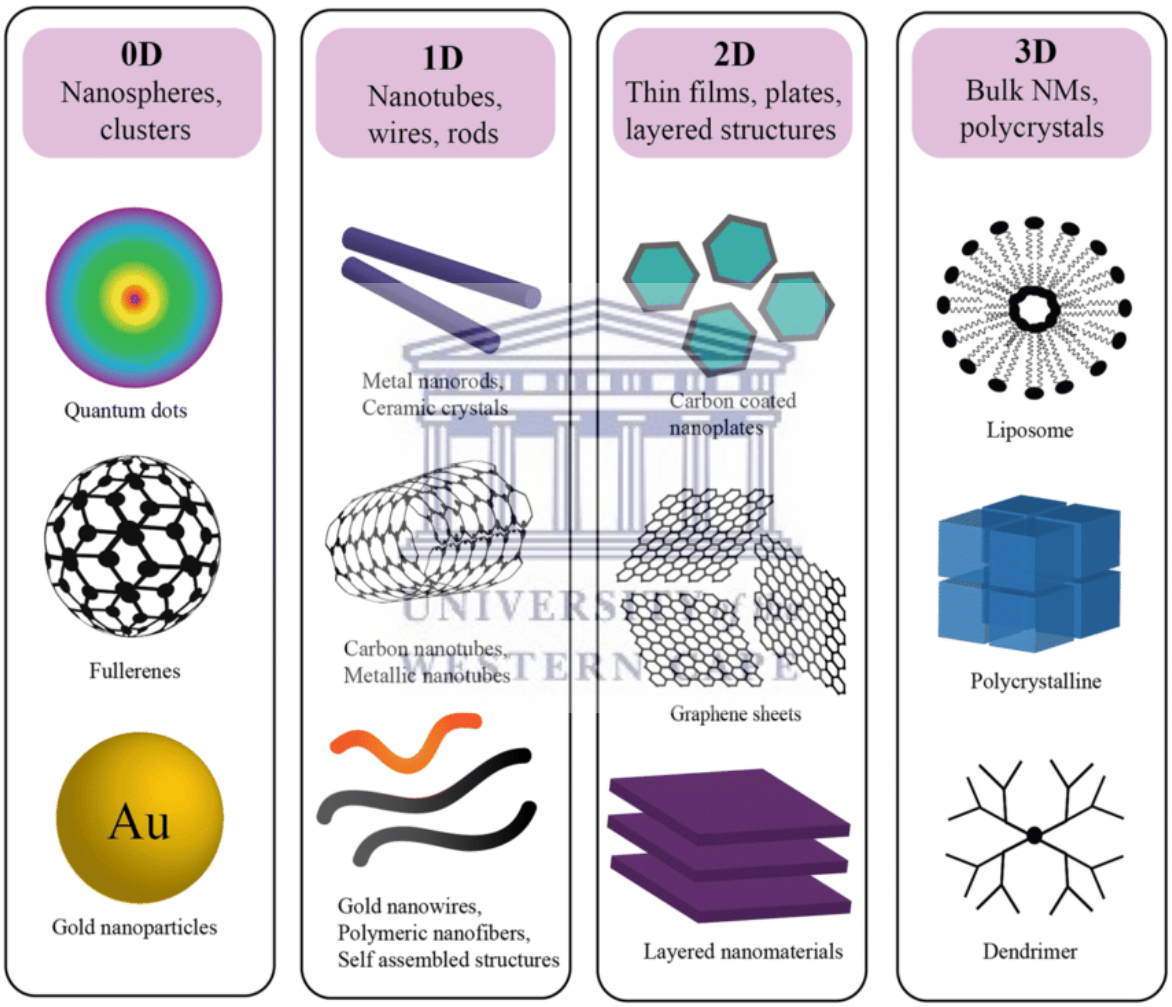


Figure 1.3: The summary of classifications of nanomaterials based on dimensional (Poh et al., 2018).

The dimensionality classification is based on nanomaterials' morphology and shape. Nanomaterials can either be zero-dimensional (0D) such as quantum dots and nanoparticles. Nanorods or nanotubes are a type of one-dimensional (1D) nanomaterial, whereas films and layers are a type of two-dimensional (2D) nanomaterial. The 0D, 1D, and 2D are mostly divided into categories based on isolated single nanoparticles. Bulk or three-dimensional (3D) nanomaterials are nanomaterials made up of several constituents. As shown in figure 1.3, nanomaterials exist in different shapes such as tubes, wires, crystals, rods, spheres, and even nanoplates and sheets (Li and Wang., 2020).

### 1.5.2. Synthesis of nanoparticles

Metallic nanoparticles can be synthesized by various methods grouped into the bottom-up or top-down approach (Abid et al., 2021). Figure 1.4 below, shows a representation of the different methods used to synthesize various nanoparticles.

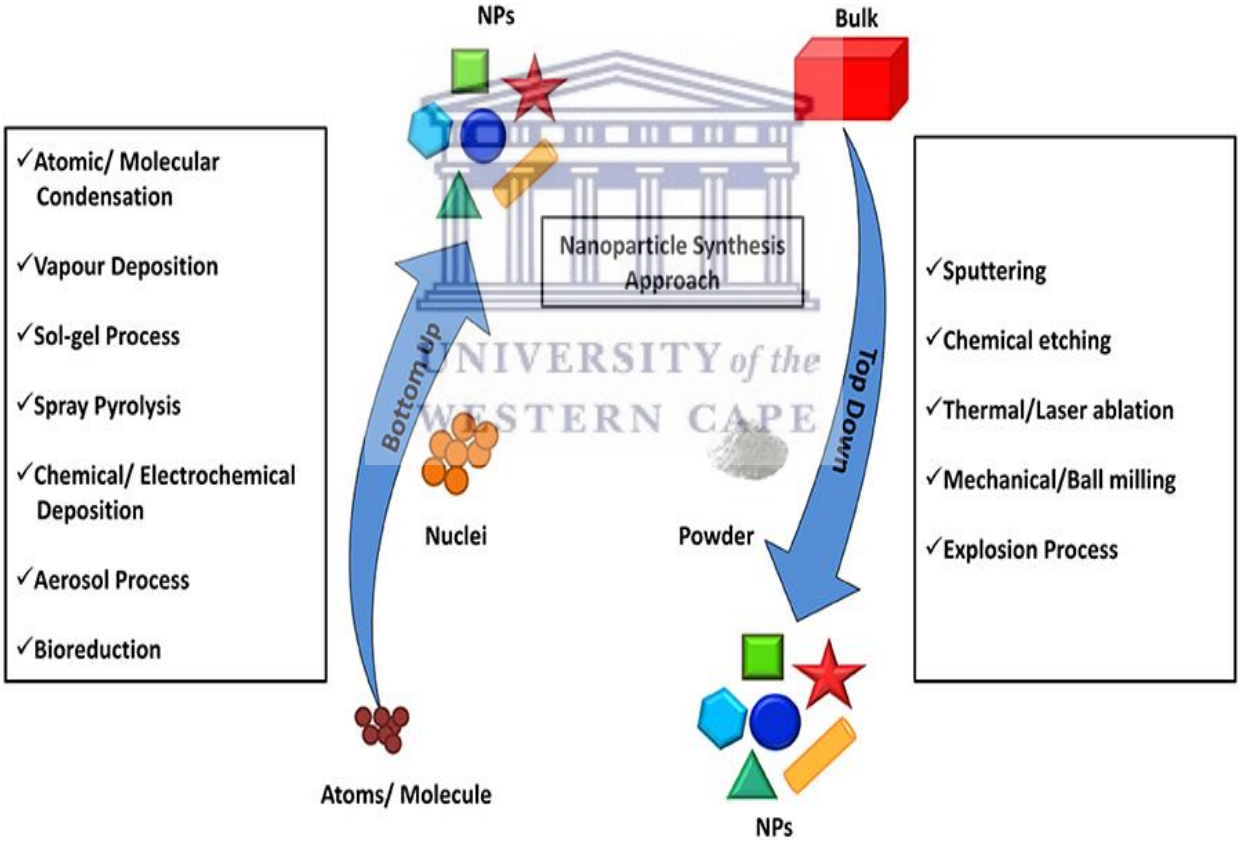


Figure 1.4: Schematic diagram for the various methods for the synthesis of nanoparticles (Ovais et al., 2017).

The top-down approach begins with a bulk structure and then, by etching off the crystal planes of the original structure, the nanosized material is obtained. Another method is grounding the bulk material into a fine powder using physical techniques like mechanical grinding or ball milling, and stabilizing chemicals are added only when necessary to prevent agglomeration (Yadav et al., 2012). The drawback of this approach is the uneven surfaces or ruptured edges of the nanomaterial, which can further affect the physiochemical properties and surface energy of the nanomaterials (Abid et al., 2021). These problems are solved by the bottom-up approach, which also offers an interesting way of synthesizing monodispersed anisotropic nanostructures (Bhol et al., 2020). The bottom-up approach has been reported to synthesize metallic nanoparticles such as AuNPs. Metallic-based nanomaterials are well known due to their wide range of applications in the biomedical field which aligns with the purpose of this project. Metallic nanoparticles are mainly used for their antibacterial properties; for instance, gold nanoparticles (AuNPs) have been used for the inhibition of toxicity and increment of therapeutic effects in cancer therapy (Sarfraz and Khan., 2021).

### 1.6. History of gold nanoparticles and their applications

Generally, the gold precious metal has a history of being used mostly in jewelry, money exchange, and as the gold standard (Zhang et al., 2015). On the other hand, gold nanoparticles (AuNPs) have been used since the Roman era (Louis and Pluchery., 2012), which has a very extensive history. The creation of ruby-red tinted glass was AuNPs' first use. The first significant accomplishment for the application of AuNPs was the production of the Lycurgus Cup glass cup made in Rome which exhibited optical properties (Figure 1.6). Written records indicated that individuals started to recognize the medieval practice of using gold with red-colored glass and further developed other gold ruby glass cups (Bayda et al., 2019). Apart from being used for decoration, gold has been reported to be already being used by the Chinese as a medicine in 2500 B.C. In India, gold was used in the form of ayurvedic medicine called “Swarna Bhasma” for the treatment of illnesses such as rheumatoid (Kashani et al., 2018). Cinnabar-gold, also known as “Makaradhwaja” has been reported to be used as an antidiabetic drug in India (Charde et al., 2019).

Figure 1.5: The image of the Roman Lycurgus Cup glass cup made in Rome during the 4th century AD which exhibits different optical properties (Das et al., 2016).

In modern days, AuNPs are applied in different industries with the biological application of AuNPs has been explored widely. Gold nanoparticles (AuNPs) have been discovered as a promising material for transporting therapeutic drugs into the target site (Connor et al., 2005). The unique features of AuNPs, particularly in the transport and release of therapeutic substances to the target location, led to their acceptance as an attractive choice for drug delivery (Skirtach et al., 2006). The therapeutic agents to be administered might be small drug molecules or big macromolecules such as proteins, DNA, or RNA, and the efficacy of their release is required for effective therapy (Rane et al., 2018).

### 1.7. Biological synthesis of Au nanoparticles

Biological synthesis is currently in the best interest due to more advantages than the other methods. This synthesis method (also part of green synthesis) releases less to no toxic substances into the environment and causes less harm to plants and animals hence it follows the sustainable development goals (SDGs) (Duan et al., 2015). The announcement of the SDGs has addressed various environmental issues. These SDGs focus on practicing cleaner production and enhancing social, environmental, and economic achievements through the management of solid waste (Tawfik et al., 2021). The biological synthesis further shows the practice that follows SDGs by having few uncomplicated synthetic stages which enable quicker nanoparticle synthesis, ease of upscale, and energy and water savings (Zhang et al., 2011).

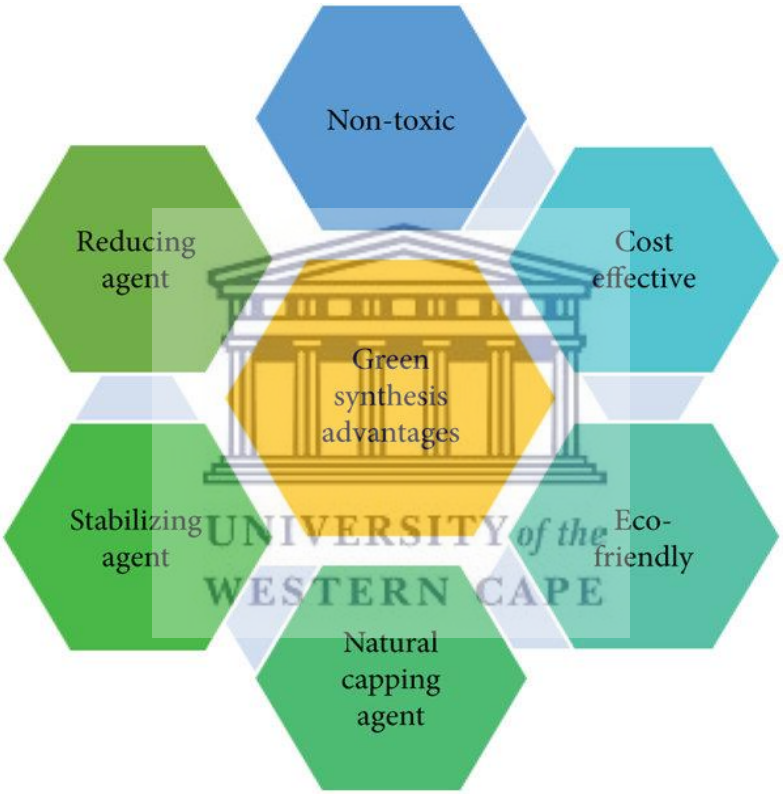


Figure 1.6: Advantages of green synthesis (Jadhav et al., 2022).

Microorganisms, enzymes, and plant extracts are the most important reducing agents in biological methods (Ghaffari-Moghaddam et al., 2014). Plants are more favorable than other biological processes for nanoparticle synthesis since they do not require the maintenance of cell cultures and are suitable for large-scale nanoparticle synthesis (Roy and Das., 2015).

### 1.7.1. Role of phytochemicals in the synthesis of AuNPs nanoparticles

Phytochemicals are naturally occurring bioorganic molecules often with high molecular weight which constitute a complex and chemically diverse group of compounds. They are naturally synthesized by plants to defend themselves against pathogens and predators (Lattanzio et al., 2009). Examples of phytochemicals are phenolics, flavonoids, terpenoids, and many others (Karthikeyan and Vidya., 2019). The role of phytochemicals in the biosynthesis of metallic nanoparticles could either be a reducing, capping, and/or stabilizing agent (Ovais et al., 2018).

#### 1.7.1.1. Role of Phenolic compounds

Phenolic compounds are secondary metabolites that are synthesized by plants through the shikimic acid and phenylpropanoid pathways (Laura et al., 2019). The effect of phenolic compounds on the synthesis of AuNPs has been investigated by Alegria and colleagues. They extracted polyphenols from tea extracts and used them on a single-step reduction of $HAuCl_4$ to form gold nanoparticles. They successfully synthesized AuNPs and reported that the phenolics acted as both reducing and capping agents (Alegria et al., 2018). AuNPs were also synthesized using hydroxycinamic (caffeic, sinapinic, and ferulic acids) and hydroxybenzoic (protocatechuic, syringic, and vanillic acids) as reducing agents of $HAuCl_4$ solution. They studied the TEM and UV-Vis spectra of the synthesized AuNPs. Different spectra and TEM images were obtained and they concluded that it is due to the different reducing power and stabilization capacity of the phenolic acids. Moreover, they reported that the higher reducing capacity of the phenolic acid used corresponds to a higher NP diameter size (Lerma-García et al., 2014). Furthermore, the reducing and stabilizing role of phenolics was investigated by Ahmad and colleagues by establishing a reaction mechanism of the AuNP synthesis using aqueous *Elaeis guineensis* leaves extract (Ahmad et al., 2019).

### 1.7.1.2. Role of flavonoids

Flavonoids are a group of aromatic compounds that are heterocyclic and contain carbonyl and phenolic as functional groups. Irfan and colleagues have extracted flavonoids from the leaves of *Elaeis guineensis* using ionic liquid-based extraction. They reported that flavonoids were one of the main compounds contained in their oil palm leaves when they investigated the total flavonoid content. Flavonoids were found to be active compounds in the reduction of gold ions into AuNPs. They attributed this potential to the hydroxyl and carbonyl groups of flavonoids which have an affinity to bind with metals and showed a chelate effect (Irfan et al., 2017). The role of flavonoids such as citrus flavonoids, diosmin (Dm), and hesperetin (Ht), was also reported to synthesize spherical AuNPs using a biogenic approach. They concluded that high concentrations of 7 mM in an alkaline solution at room temperature were able to reduce the gold salt and yielded uniform spherical AuNPs (Sierra et al., 2016).

### 1.7.1.3. Role of terpenoids

Terpenoids are a group of plant secondary metabolites that contain C= 5, 10, 15, 20…, n > 40 carbon units (Proshkina et al., 2020). Vilas and associates have used the essential oil from *Coleus aromaticus* to biosynthesize Au and Au-Ag alloy nanoparticles for the evaluation of the antibacterial activity. They reported that terpenoids from the extracted essential oil have played a vital role in the reduction and stabilization of the synthesized nanoparticles (Vilas et al., 2016).



### 1.7.2. Mechanism involved in the phytochemical synthesis of AuNPs

In 1857, Michael Faraday proposed a general chemical reduction method for the reduction of gold using a specific metal salt, a suitable stabilizer which led to the product of metallic nanoparticles dispersed in an aqueous solvent (Hammami and Alabdallah., 2021). The discovery of this technique led to Turkevich's experiments to establish a standard growth mechanism for the synthesis of AuNPs which has stages 4 stages (Figure 1.5).

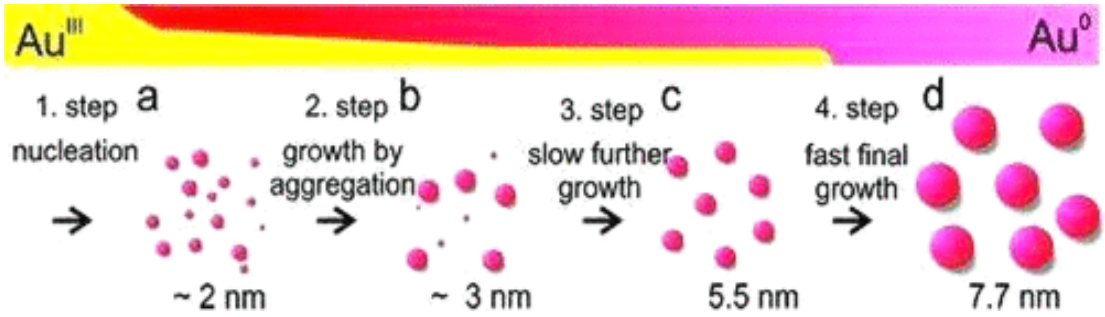


Figure 1.7: The mechanism of nucleation and growth of nanoparticles in the solution proposed by Turkevich (Turkevich et al., 1951).

This mechanism shows the reduction of precursors ($Au^{3+}$) into $Au^0$ in the presence of a reducing agent. The first step involves the formation of seeds by the coalescence of nuclei and aggregation of seeds for growth (steps 1 and 2). A further monomer attachment results in the slow growth of the nanoparticles at step 3. The final step involves the reduction of the remaining precursor on the surface of the grown particle leading to the final larger particle size. (Polte et al., 2010). This proposed growth mechanism led to the use of different reducing agents such as biological agents.

### 1.8. Antimicrobial activity of gold nanoparticles

The antimicrobial activity of AuNPs is amongst the most investigated application of gold nanoparticles (Nadeem et al., 2017). This activity is attributed to their ability to have a functionalized surface, smaller size, and be biologically inert (Brandelli et al., 2017). The exact mechanism for the antimicrobial action of gold nanoparticles is poorly understood (Godoy-Gallardo et al., 2021). The nano-size of AuNPs could be one of the possibilities because they are very small than the bacterial cell which makes them penetrate the cell easily and cause cellular death (Yeo et al., 2022; Balderrama-González et al., 2021). Moreover, the cell wall composition plays a role in the antimicrobial property of AuNPs. On gram-negative bacteria, AuNPs show the highest activity than gram-positive bacteria (Nadeem et al., 2017). Gold nanoparticles exhibit different physical and chemical properties which result to advance research of their application (Zhang et al., 2015).

Table 1: The summary of gold nanoparticles aiding antimicrobial activity.

| Number | Property | References |
|---|---|---|
| 1 | The high surface-volume ratio increased surface chemical reactivity and enhanced the chemisorption of CO and H2 molecules. | Zhang et al., 2015 |
| 2 | Possess dielectric function, electrical conductivity, and inert property to oxidation. | Zhang et al., 2015 |
| 3 | Surface plasmon resonance (SPR) property allows applications as sensors for the detection of biological targets and many others. | Daniel and Astruc., 2004 |
| 4 | The surface of AuNPs can also be modified using different coating agents with different functionalities making them very useful in biology and medicine. | Zhang et al., 2015 |



### 1.8.1. Antifungal Effect of Gold Nanoparticle

Some researchers investigated the antifungal effect of AuNPs, which appears to be size, shape, and concentration-dependent. López-Lorente and colleagues observed the effect that the synthesis, purification, and growth determination methods on the antifungal activity of AuNPs. They concluded that the antifungal activity of AuNPs depends only on the growth determination method and not purification (López-Lorente et al., 2019). Green AuNPs having a size between 20-40 nm were synthesized using algae extract and they exhibited antifungal activity against *C. tropicalis*, *C. glabrata*, and *C. albicans* (Gürsoy et al., 2021).

### 1.8.2. Antibacterial Effect of Green Synthesized Gold Nanoparticles

Literature has shown that AuNPs synthesized using natural compounds extracted from plants have antibacterial properties. For instance, Akintelu and colleagues (2021) have synthesized spherical AuNPs of 18-38 nm using *Garcinia kola* Pulp extracts as the reducing agent, which showed a maximum inhibition zone on *Escherichia coli and* least on *Staphylococcus aureus* (Akintelu et al., 2021). Hamelian and coauthors synthesized 50-60 nm AuNPs using *Pistacia*

*Atlantica* (leave and fruit) extract to reduce $HAuCl_4 \times H_2O$. These AuNPs showed antimicrobial activity in *Escherichia coli*, *Pseudomonas aeruginosa* (Gram-negative bacteria), *Staphylococcus aureus*, and *Bacillus subtilis* (gram-positive) (Hamelian et al., 2018). The green synthesized AuNPs are reported to have more efficient antibacterial activity against certain bacteria strains than the chemically synthesized AuNPs (Zhang et al., 2015). This could result from the extracts alone, AuNPs, or their combination. Some extracts, like the plant *Aloe vera*, have antibacterial activity (Danish et al., 2020). The antibacterial activity could be due to the synergistic effect of the combination of AuNPs and extracts (Zhang et al., 2015).

### 1.8.3. Antimicrobial activity of gold nanoparticles combined with antibiotics

Gold nanoparticles are reported to have no specific antimicrobial activity but rather they could enhance the antimicrobial efficacy of other molecules (Gu et al., 2021). Nejati and coauthors reported AuNPs as drug-delivery vehicles because of their unique physicochemical properties (Nejati et al., 2021). This results in AuNPs being combined with antibiotics to improve the antimicrobial efficiency to fight multidrug-resistant bacteria (Zhang et al., 2015). Shah and colleagues have stabilized AuNPs with 20-40 nm size using ceftriaxone and used atomic force spectroscopy to analyze the antimicrobial action on *E.coli*. The results showed the minimum inhibitory concentration (MIC) values of ceftriaxone-AuNPs conjugates to be 4.3 ± 0.57 µg/mL while unconjugated AuNPs are 73 ± 1.9 µg/mL. This shows that the ceftriaxone-AuNPs require a very small concentration to inhibit *E.coli* hence showing enhanced antimicrobial activity (Shah et al., 2014).



### 1.8.4. Gold Nanoparticles Used as Delivery Vehicles for Antibiotics

AuNPs have been explored for use as drug delivery agents of antibiotic molecules. AuNPs can interact with antibiotics with even weak forces such as van der Waals interaction (Zhang et al., 2015). Dul and colleagues have used antigen-specific immunotherapy using AuNPs because of their potential to deliver a peptide autoantigen in conjunction with pro-tolerogenic elements for the treatment of type 1 diabetes. They reported that the AuNPs remained stable when moving through microneedles and delivered to human skin and diffuse up to the epidermic layer (Dul et al., 2019).

### 1.9.1. Hypothesis

The *Artemisia annua* aqueous extract contains phytochemicals that can reduce the Gold (III) chloride hydrate ($HAuCl_4 \bullet XH_2O$) precursor into gold nanoparticles (AuNPs). The biosynthesized AuNPs have antimicrobial activity against common bacterial strains responsible for causing resistant infections.

### 1.9.2. Aim and objectives

The main aim of this project is to synthesize gold nanoparticles (AuNPs) from an aqueous extract of *Artemisia annua* and optimize the synthesis conditions. The antimicrobial activity of the optimized AuNPs will be investigated against bacterial strains responsible for resistant infections.

**Research objectives**

- To synthesis of AuNPs using the bioreduction method will be done by reacting the gold (III) chloride hydrate ($HAuCl_4 \bullet XH_2O$) precursors with *Artemisia annua* plant extract.
- To carry out optimization by changing reaction parameters such as reactants concentrations, incubation time, temperature, and pH.
- To characterize the biosynthesized AuNPs and *Artemisia annua* using FTIR, DLS, UV-Vis, XRD, and HRTEM to confirm the success in the production of AuNPs using optimized conditions.
- To investigate the antimicrobial activity of the synthesized *A.annua*-AuNPs and *Artemisia annua* aqueous extract using Gram-positive strains, *Staphylococcus aureus* (ATCC 25923), *Staphylococcus epidermidis* (ATCC 12228), and *Methicillin-resistant Staphylococcus aureus* (MRSA (ATCC 33591)) with a total of 3 Gram-negative strains *Klebsiella pneumoniae* (ATCC 13883), *Escherichia coli* (ATCC 35281), and *Pseudomonas aeruginosa* (ATCC 27853).

**References**

Abid, N., Khan, A.M., Shujait, S., Chaudhary, K., Ikram, M., Imran, M., Haider, J., Khan, M., Khan, Q. and Maqbool, M., 2021. Synthesis of nanomaterials using various top-down and bottom-up approaches, influencing factors, advantages, and disadvantages: A review. Advances in Colloid and Interface Science, p.102597.

Abubakar, I., Irvine, L., Aldus, C.F., Wyatt, G.M., Fordham, R., Schelenz, S., Shepstone, L., Howe, A., Peck, M. and Hunter, P.R., 2007. A systematic review of the clinical, public health and cost-effectiveness of rapid diagnostic tests for the detection and identification of bacterial intestinal pathogens in faeces and food. Health technology assessment (Winchester, England), 11(36), pp.1-216.

Ahmad, T., Bustam, M.A., Irfan, M., Moniruzzaman, M., Asghar, H.M.A. and Bhattacharjee, S., 2019. Mechanistic investigation of phytochemicals involved in green synthesis of gold nanoparticles using aqueous Elaeis guineensis leaves extract: Role of phenolic compounds and flavonoids. Biotechnology and applied biochemistry, 66(4), pp.698-708.

Ahmed, A.A., Zakaria, Z., Ali, M.H., Pusppanathan, J., Mhji, S.Z.M., Noor, A.M., Rahiman, M.H.F., Hassan, M.K.A., Safar, M.J.A. and Salleh, A.F., 2020, May. An overview of medical applications in meningitis detection. In IOP conference series: materials science and engineering (Vol. 864, No. 1, p. 012156). IOP Publishing.

Ajayan, P.M. and Zhou, O.Z., 2001. Applications of carbon nanotubes. Carbon nanotubes, pp.391-425.

Akintelu, S.A., Olugbeko, S.C. and Folorunso, A.S., 2020. A review on synthesis, optimization, characterization and antibacterial application of gold nanoparticles synthesized from plants. International Nano Letters, 10(4), pp.237-248.

Akintelu, S.A., Yao, B. and Folorunso, A.S., 2021. Green synthesis, characterization, and antibacterial investigation of synthesized gold nanoparticles (AuNPs) from Garcinia kola pulp extract. Plasmonics, 16(1), pp.157-165.

Alegria, E.C., Ribeiro, A.P., Mendes, M., Ferraria, A.M., Rego, A.M.B.D. and Pombeiro, A.J., 2018. Effect of phenolic compounds on the synthesis of gold nanoparticles and its catalytic activity in the reduction of nitro compounds. Nanomaterials, 8(5), p.320.

Ali, M.R., Wu, Y. and El-Sayed, M.A., 2019. Gold-nanoparticle-assisted plasmonic photothermal therapy advances toward clinical application. The Journal of Physical Chemistry C, 123(25), pp.15375-15393.

Allen, M., Bridle, G. and Briten, E., 2015. Life under the Microscope: Children's Ideas about Microbes. *Primary Science*, *136*, pp.35-38.

Ananthakumar, S. and Babu, S.M., 2018. Progress on synthesis and applications of hybrid perovskite semiconductor nanomaterials—A review. Synthetic Metals, 246, pp.64-95.

Ashley, E.A., Dhorda, M., Fairhurst, R.M., Amaratunga, C., Lim, P., Suon, S., Sreng, S., Anderson, J.M., Mao, S., Sam, B. and Sopha, C., 2014. Spread of artemisinin resistance in Plasmodium falciparum malaria. New England Journal of Medicine, 371(5), pp.411-423.

Aslam, I., Fleischer, A. and Feldman, S., 2015. Emerging drugs for the treatment of acne. Expert opinion on emerging drugs, 20(1), pp.91-101.

Aweeka, F.T. and German, P.I., 2008. Clinical pharmacology of artemisinin-based combination therapies. Clinical pharmacokinetics, 47, pp.91-102.

Ayukekbong, J.A., Ntemgwa, M. and Atabe, A.N., 2017. The threat of antimicrobial resistance in developing countries: causes and control strategies. *Antimicrobial Resistance & Infection Control*, *6*(1), pp.1-8.

Balderrama-González, A.S., Piñón-Castillo, H.A., Ramírez-Valdespino, C.A., Landeros-Martínez, L.L., Orrantia-Borunda, E. and Esparza-Ponce, H.E., 2021. Antimicrobial resistance and inorganic nanoparticles. International Journal of Molecular Sciences, 22(23), p.12890.

Basavegowda, N., Idhayadhulla, A. and Lee, Y.R., 2014. Preparation of Au and Ag nanoparticles using Artemisia annua and their in vitro antibacterial and tyrosinase inhibitory activities. *Materials Science and Engineering: C*, *43*, pp.58-64.

Bayda, S., Adeel, M., Tuccinardi, T., Cordani, M. and Rizzolio, F., 2019. The history of nanoscience and nanotechnology: from chemical–physical applications to nanomedicine. Molecules, 25(1), p.112.

Bhol, P., Bhavya, M.B., Swain, S., Saxena, M. and Samal, A.K., 2020. Modern chemical routes for the controlled synthesis of anisotropic bimetallic nanostructures and their application in catalysis. Frontiers in Chemistry, 8, p.357.

Bilia, A.R., Santomauro, F., Sacco, C., Bergonzi, M.C. and Donato, R., 2014. Essential oil of Artemisia annua L.: an extraordinary component with numerous antimicrobial properties. *Evidence-based complementary and alternative medicine*, *2014*.

Brandelli, A., Ritter, A.C. and Veras, F.F., 2017. Antimicrobial activities of metal nanoparticles. In Metal nanoparticles in pharma (pp. 337-363). Springer, Cham.

Byarugaba, D.K., 2004. Antimicrobial resistance in developing countries and responsible risk factors. *International journal of antimicrobial agents*, *24*(2), pp.105-110.

Cancio, L.C., 2021. Topical antimicrobial agents for burn wound care: history and current status. Surgical Infections, 22(1), pp.3-11.

Cassini, A., Högberg, L.D., Plachouras, D., Quattrocchi, A., Hoxha, A., Simonsen, G.S., Colomb-Cotinat, M., Kretzschmar, M.E., Devleesschauwer, B., Cecchini, M. and Ouakrim, D.A., 2019. Attributable deaths and disability-adjusted life-years caused by infections with antibiotic-resistant bacteria in the EU and the European Economic Area in 2015: a population-level modelling analysis. The Lancet infectious diseases, 19(1), pp.56-66.

Chan, E., Tan, M., Xin, J., Sudarsanam, S. and Johnson, D.E., 2010. Interactions between traditional Chinese medicines and Western. Curr Opin Drug Discov Devel, 13(1), pp.50-65.

Charde, V.A., Patel, K.P., Kaur, H., Jagtap, C., Nariya, M., Patgiri, B., Murthy, S.N. and Prajapati, P., 2019. Evaluation of Antihyperglycemic and Hypoglycemic Activities of Shadguna Makaradhwaja and Guduchi Ghana in Swiss Albino Mice.



Chaudhry, Q. and Castle, L., 2011. Food applications of nanotechnologies: an overview of opportunities and challenges for developing countries. *Trends in Food Science & Technology*, *22*(11), pp.595-603.

Cheng, G., Dai, M., Ahmed, S., Hao, H., Wang, X. and Yuan, Z., 2016. Antimicrobial drugs in fighting against antimicrobial resistance. Frontiers in Microbiology, 7, p.470.

Connor, E.E., Mwamuka, J., Gole, A., Murphy, C.J. and Wyatt, M.D., 2005. Gold nanoparticles are taken up by human cells but do not cause acute cytotoxicity. *Small*, *1*(3), pp.325-327.

Dadgostar, P., 2019. Antimicrobial resistance: implications and costs. Infection and drug resistance, 12, p.3903.

Daniel, M.C. and Astruc, D., 2004. Gold nanoparticles: assembly, supramolecular chemistry, quantum-size-related properties, and applications toward biology, catalysis, and nanotechnology. Chemical reviews, 104(1), pp.293-346.

Danish, P., Ali, Q., Hafeez, M.M. and Malik, A., 2020. Antifungal and antibacterial activity of aloe vera plant extract. Biological and Clinical Sciences Research Journal, 2020(1).

Dankovich, T.A. and Gray, D.G., 2011. Bactericidal paper impregnated with silver nanoparticles for point-of-use water treatment. *Environmental science & technology*, *45*(5), pp.1992-1998.

Das, G., Coluccio, M.L., Alrasheed, S., Giugni, A., Allione, M., Torre, B., Perozziello, G., Candeloro, P. and Di Fabrizio, E., 2016. Plasmonic nanostructures for the ultrasensitive detection of biomolecules. La Rivista del Nuovo Cimento, 39(11), pp.547-586.

Doron, S. and Gorbach, S.L., 2008. Bacterial infections: overview. International Encyclopedia of Public Health, p.273.

Duan, H., Wang, D. and Li, Y., 2015. Green chemistry for nanoparticle synthesis. Chemical Society Reviews, 44(16), pp.5778-5792.

Dul, M., Nikolic, T., Stefanidou, M., McAteer, M.A., Williams, P., Mous, J., Roep, B.O., Kochba, E., Levin, Y., Peakman, M. and Wong, F.S., 2019. Conjugation of a peptide autoantigen to gold nanoparticles for intradermally administered antigen specific immunotherapy. International Journal of Pharmaceutics, 562, pp.303-312.

Eagye, K.J., Nicolau, D.P. and Kuti, J.L., 2009, February. Impact of superinfection on hospital length of stay and costs in patients with ventilator-associated pneumonia. In Seminars in Respiratory and Critical Care Medicine (Vol. 30, No. 01, pp. 116-123). © Thieme Medical Publishers.

Ealia, S.A.M. and Saravanakumar, M.P., 2017, November. A review on the classification, characterisation, synthesis of nanoparticles and their application. In IOP conference series: materials science and engineering (Vol. 263, No. 3, p. 032019). IOP Publishing.

Edwards, S.E., da Costa Rocha, I., Williamson, E.M. and Heinrich, M., 2015. Lemon Balm Melissa officinalis L. Phytopharmacy: An Evidence-Based Guide to Herbal Medicinal Products, p.242.

Efferth, T., 2017, October. From ancient herb to modern drug: Artemisia annua and artemisinin for cancer therapy. In Seminars in cancer biology (Vol. 46, pp. 65-83). Academic Press.

Feng, X., Cao, S., Qiu, F. and Zhang, B., 2020. Traditional application and modern pharmacological research of Artemisia annua L. *Pharmacology & Therapeutics*, p.107650.

Feynman, R.P., 1960. An invitation to enter a new field of physics. *Int. J. Eng. Sci*, *23*(8).

Fluit, A.C., Visser, M.R. and Schmitz, F.J., 2001. Molecular detection of antimicrobial resistance. *Clinical microbiology reviews*, *14*(4), pp.836-871.

Fokunang, C.N., Ndikum, V., Tabi, O.Y., Jiofack, R.B., Ngameni, B., Guedje, N.M., Tembe-Fokunang, E.A., Tomkins, P., Barkwan, S., Kechia, F. and Asongalem, E., 2011. Traditional medicine: past, present and future research and development prospects and integration in the National Health System of Cameroon. African journal of traditional, complementary and alternative medicines, 8(3).

Fuentes, E., Fuentes, M., Alarcón, M. and Palomo, I., 2017. Immune system dysfunction in the elderly. Anais da Academia Brasileira de Ciências, 89, pp.285-299.

Ghaffari-Moghaddam, M., Hadi-Dabanlou, R., Khajeh, M., Rakhshanipour, M. and Shameli, K., 2014. Green synthesis of silver nanoparticles using plant extracts. Korean Journal of Chemical Engineering, 31(4), pp.548-557.

Godoy-Gallardo, M., Eckhard, U., Delgado, L.M., de Roo Puente, Y.J., Hoyos-Nogués, M., Gil, F.J. and Perez, R.A., 2021. Antibacterial approaches in tissue engineering using metal ions and nanoparticles: From mechanisms to applications. Bioactive Materials, 6(12), pp.4470-4490.

Gu, X., Xu, Z., Gu, L., Xu, H., Han, F., Chen, B. and Pan, X., 2021. Preparation and antibacterial properties of gold nanoparticles: A review. Environmental Chemistry Letters, 19(1), pp.167-187.



Gürsoy, N., Öztürk, B.Y. and Dağ, İ., 2021. Synthesis of intracellular and extracellular gold nanoparticles with a green machine and its antifungal activity. Turkish Journal of Biology, 45(2), pp.196-213.

Hamelian, M., Hemmati, S., Varmira, K. and Veisi, H., 2018. Green synthesis, antibacterial, antioxidant and cytotoxic effect of gold nanoparticles using Pistacia Atlantica extract. Journal of the Taiwan Institute of Chemical Engineers, 93, pp.21-30.

Hammami, I. and Alabdallah, N.M., 2021. Gold nanoparticles: Synthesis properties and applications. Journal of King Saud University-Science, 33(7), p.101560.

Hart, C.A. and Kariuki, S., 1998. Antimicrobial resistance in developing countries. *Bmj*, *317*(7159), pp.647-650.

Havlickova, B., Czaika, V.A. and Friedrich, M., 2008. Epidemiological trends in skin mycoses worldwide. Mycoses, 51, pp.2-15.

Holmes, E.C., Rambaut, A. and Andersen, K.G., 2018. Pandemics: spend on surveillance, not prediction.

Honce, R. and Schultz-Cherry, S., 2019. Impact of obesity on influenza A virus pathogenesis, immune response, and evolution. Frontiers in immunology, 10, p.1071.

Hyeon, T., Manna, L. and Wong, S.S., 2015. Sustainable nanotechnology. Chemical Society Reviews, 44(16), pp.5755-5757.

Irfan, M., Moniruzzaman, M., Ahmad, T., Mandal, P.C., Bhattacharjee, S. and Abdullah, B., 2017. Ionic liquid based extraction of flavonoids from Elaeis guineensis leaves and their applications for gold nanoparticles synthesis. *Journal of Molecular Liquids*, *241*, pp.270-278.

Jadhav, V., Bhagare, A., Ali, I.H., Dhayagude, A., Lokhande, D., Aher, J., Jameel, M. and Dutta, M., 2022. Role of Moringa oleifera on green synthesis of metal/metal oxide nanomaterials. *Journal of Nanomaterials*, *2022*.

Jana, S., Iram, S., Thomas, J., Hayat, M.Q., Pannecouque, C. and Dehaen, W., 2017. Application of the triazolization reaction to afford dihydroartemisinin derivatives with anti-HIV activity. Molecules, 22(2), p.303.

Karakonstantis, S. and Kalemaki, D., 2019. Antimicrobial overuse and misuse in the community in Greece and link to antimicrobial resistance using methicillin-resistant S. aureus as an example. Journal of Infection and Public Health, 12(4), pp.460-464.

Karthikeyan, G. and Vidya, A., 2019. Phytochemical analysis, antioxidant and antibacterial activity of pomegranate peel. Research Journal of Life Science, Bioinformatics, Pharmaceutical and Chemical Science, 5(1).

Kashani, A.S., Kuruvinashetti, K., Beauet, D., Badilescu, S., Piekny, A. and Packirisamy, M., 2018. Enhanced internalization of indian ayurvedic swarna bhasma (Gold Nanopowder) for effective interaction with human cells. Journal of Nanoscience and Nanotechnology, 18(10), pp.6791-6798.

Khalid, M., Kayani, S.I., Jan, F., Ullah, A. and Tang, K., 2019. Biological activities of artemisinins beyond anti-malarial: a review. Tropical Plant Biology, 12(4), pp.231-243.

Khamesipour, F., Lankarani, K.B., Honarvar, B. and Kwenti, T.E., 2018. A systematic review of human pathogens carried by the housefly (Musca domestica L.). BMC public health, 18(1), pp.1-15.

Klayman, D.L., 1993. Artemisia annua: from weed to respectable antimalarial plant.

Kolahalam, L.A., Viswanath, I.K., Diwakar, B.S., Govindh, B., Reddy, V. and Murthy, Y.L.N., 2019. Review on nanomaterials: Synthesis and applications. Materials Today: Proceedings, 18, pp.2182-2190.

Krishnaswamy, K., Vali, H. and Orsat, V., 2014. Value-adding to grape waste: Green synthesis of gold nanoparticles. *Journal of Food Engineering*, *142*, pp.210-220

Krol, S., Macrez, R., Docagne, F., Defer, G., Laurent, S., Rahman, M., Hajipour, M.J., Kehoe, P.G. and Mahmoudi, M., 2013. Therapeutic benefits from nanoparticles: the potential significance of nanoscience in diseases with compromise to the blood brain barrier. Chemical reviews, 113(3), pp.1877-1903.

Kumar, A., Kumar, A. and Patel, H., 2018. Role of microbes in phosphorus availability and acquisition by plants. International journal of current microbiology and applied Sciences, 7(5), pp.1344-1347.

Kumar, V.G., Gokavarapu, S.D., Rajeswari, A., Dhas, T.S., Karthick, V., Kapadia, Z., Shrestha, T., Barathy, I.A., Roy, A. and Sinha, S., 2011. Facile green synthesis of gold nanoparticles using leaf extract of antidiabetic potent Cassia auriculata. *Colloids and Surfaces B: Biointerfaces*, *87*(1), pp.159-163.



Lattanzio, V., Kroon, P.A., Quideau, S. and Treutter, D., 2009. Plant phenolics—secondary metabolites with diverse functions. Recent advances in polyphenol research, 1, pp.1-35.

Laura, A., Moreno-Escamilla, J.O., Rodrigo-García, J. and Alvarez-Parrilla, E., 2019. Phenolic compounds. In *Postharvest physiology and biochemistry of fruits and vegetables* (pp. 253-271). Woodhead publishing.

Lerma-García, M., Ávila, M., Simó-Alfonso, E.F., Ríos, Á. and Zougagh, M., 2014. Synthesis of gold nanoparticles using phenolic acids and its application in catalysis. *J. Mater. Environ. Sci*, *5*(6), pp.1919-1926.

Levy, S.B. and Marshall, B., 2004. Antibacterial resistance worldwide: causes, challenges and responses. Nature medicine, 10(Suppl 12), pp.S122-S129.

Li, S., Zhu, Q., Luo, J., Shu, Y., Guo, K., Xie, J., Xiao, F. and He, S., 2021. Application progress of deinococcus radiodurans in biological treatment of radioactive uranium-containing wastewater. Indian Journal of Microbiology, 61(4), pp.417-426.

Li, X. and Wang, J., 2020. One-dimensional and two-dimensional synergized nanostructures for high-performing energy storage and conversion. InfoMat, 2(1), pp.3-32.

Li, Z., Lu, G. and Meng, G., 2019. Pathogenic fungal infection in the lung. Frontiers in immunology, 10, p.1524.

Long, J.S., Mistry, B., Haslam, S.M. and Barclay, W.S., 2019. Host and viral determinants of influenza A virus species specificity. Nature Reviews Microbiology, 17(2), pp.67-81.

López-Lorente, Á.I., Cárdenas, S. and González-Sánchez, Z.I., 2019. Effect of synthesis, purification and growth determination methods on the antibacterial and antifungal activity of gold nanoparticles. Materials Science and Engineering: C, 103, p.109805.

Louis C, Pluchery O. Gold Nanoparticles for Physics, Chemistry and Biology. London: Imperial College Press; 2012.

Manca, R., Bombillar, F., Glomski, C. and Pica, A., 2022. Obesity and immune system impairment: A global problem during the COVID-19 pandemic. International Journal of Risk & Safety in Medicine, (Preprint), pp.1-16.

Manohar, P., Madurantakam Royam, M., Loh, B., Bozdogan, B., Nachimuthu, R. and Leptihn, S., 2022. Synergistic Effects of Phage–Antibiotic Combinations against Citrobacter amalonaticus. ACS infectious diseases, 8(1), pp.59-65.

Mogensen, T.H., 2009. Pathogen recognition and inflammatory signaling in innate immune defenses. Clinical microbiology reviews, 22(2), pp.240-273.

Nadeem, M., Abbasi, B.H., Younas, M., Ahmad, W. and Khan, T., 2017. A review of the green syntheses and anti-microbial applications of gold nanoparticles. Green Chemistry Letters and Reviews, 10(4), pp.216-227.

Nair, M.S., Huang, Y., Fidock, D.A., Towler, M.J. and Weathers, P.J., 2022. Artemisia annua L. hot-water extracts show potent activity in vitro against Covid-19 variants including delta. Journal of Ethnopharmacology, 284, p.114797.

Nejati, K., Dadashpour, M., Gharibi, T., Mellatyar, H. and Akbarzadeh, A., 2021. Biomedical applications of functionalized gold nanoparticles: a review. Journal of Cluster Science, pp.1-16.

Nigam, M., Atanassova, M., Mishra, A.P., Pezzani, R., Devkota, H.P., Plygun, S., Salehi, B., Setzer, W.N. and Sharifi-Rad, J., 2019. Bioactive compounds and health benefits of Artemisia species. Natural product communications, 14(7), p.1934578X19850354.

Nosten, F. and White, N.J., 2007. Artemisinin-based combination treatment of falciparum malaria. *Defining and Defeating the Intolerable Burden of Malaria III: Progress and Perspectives: Supplement to Volume 77 (6) of American Journal of Tropical Medicine and Hygiene*.

Okeke, I.N., Laxminarayan, R., Bhutta, Z.A., Duse, A.G., Jenkins, P., O'Brien, T.F., Pablos-Mendez, A. and Klugman, K.P., 2005. Antimicrobial resistance in developing countries. Part I: recent trends and current status. *The Lancet infectious diseases*, *5*(8), pp.481-493.

Okeke, N.E., Adetunji, C.O., Nwankwo, W., Ukhurebor, K.E., Makinde, A.S. and Panpatte, D.G., 2021. A critical review of microbial transport in effluent waste and sewage sludge treatment. Microbial Rejuvenation of Polluted Environment: Volume 3, pp.217-238.

Olliaro, P.L. and Taylor, W.R., 2004. Developing artemisinin based drug combinations for the treatment of drug resistant falciparum malaria: A review. *Journal of postgraduate medicine*, *50*(1), p.40.

Osonga, F.J., Akgul, A., Yazgan, I., Akgul, A., Eshun, G.B., Sakhaee, L. and Sadik, O.A., 2020. Size and shape-dependent antimicrobial activities of silver and gold nanoparticles: A model study as potential fungicides. Molecules, 25(11), p.2682.

Ovais, M., Khalil, A.T., Islam, N.U., Ahmad, I., Ayaz, M., Saravanan, M., Shinwari, Z.K. and Mukherjee, S., 2018. Role of plant phytochemicals and microbial enzymes in biosynthesis of metallic nanoparticles. Applied microbiology and biotechnology, 102(16), pp.6799-6814.

Ovais, M., Raza, A., Naz, S., Islam, N.U., Khalil, A.T., Ali, S., Khan, M.A. and Shinwari, Z.K., 2017. Current state and prospects of the phytosynthesized colloidal gold nanoparticles and their applications in cancer theranostics. Applied microbiology and biotechnology, 101(9), pp.3551-3565.

Pal, M., Berhanu, G., Desalegn, C. and Kandi, V., 2020. Severe acute respiratory syndrome coronavirus-2 (SARS-CoV-2): an update. Cureus, 12(3).

Pangrazzi, L., Balasco, L. and Bozzi, Y., 2020. Oxidative stress and immune system dysfunction in autism spectrum disorders. International journal of molecular sciences, 21(9), p.3293.

Parsonage, B., Hagglund, P.K., Keogh, L., Wheelhouse, N., Brown, R.E. and Dancer, S.J., 2017. Control of antimicrobial resistance requires an ethical approach. Frontiers in microbiology, 8, p.2124.

Poh, T.Y., Ali, N., Mac Aogáin, M., Kathawala, M.H., Setyawati, M.I., Ng, K.W. and Chotirmall, S.H., 2018. Inhaled nanomaterials and the respiratory microbiome: clinical, immunological and toxicological perspectives. Particle and fibre toxicology, 15(1), pp.1-16.

Polte, J., Ahner, T.T., Delissen, F., Sokolov, S., Emmerling, F., Thünemann, A.F. and Kraehnert, R., 2010. Mechanism of gold nanoparticle formation in the classical citrate synthesis method derived from coupled in situ XANES and SAXS evaluation. Journal of the American Chemical Society, 132(4), pp.1296-1301.

Proshkina, E., Plyusnin, S., Babak, T., Lashmanova, E., Maganova, F., Koval, L., Platonova, E., Shaposhnikov, M. and Moskalev, A., 2020. Terpenoids as potential geroprotectors. *Antioxidants*, *9*(6), p.529.

Prow, T.W., Grice, J.E., Lin, L.L., Faye, R., Butler, M., Becker, W., Wurm, E.M., Yoong, C., Robertson, T.A., Soyer, H.P. and Roberts, M.S., 2011. Nanoparticles and microparticles for skin drug delivery. *Advanced drug delivery reviews*, *63*(6), pp.470-491.

Punjataewakupt, A., Napavichayanun, S. and Aramwit, P., 2019. The downside of antimicrobial agents for wound healing. European Journal of Clinical Microbiology & Infectious Diseases, 38(1), pp.39-54.

Qiu, L., Zhu, N., Feng, Y., Michaelides, E.E., Żyła, G., Jing, D., Zhang, X., Norris, P.M., Markides, C.N. and Mahian, O., 2020. A review of recent advances in thermophysical properties at the nanoscale: From solid state to colloids. Physics Reports, 843, pp.1-81.

Rane, A.V., Kanny, K., Abitha, V.K. and Thomas, S., 2018. Methods for synthesis of nanoparticles and fabrication of nanocomposites. In *Synthesis of inorganic nanomaterials* (pp. 121-139). Woodhead Publishing.

Rao, Y., Inwati, G.K. and Singh, M., 2017. Green synthesis of capped gold nanoparticles and their effect on Gram-positive and Gram-negative bacteria. Future science OA, 3(4), p.FSO239.

Roy, S. and Das, T.K., 2015. Plant mediated green synthesis of silver nanoparticles-A. Int. J. Plant Biol. Res, 3, pp.1044-1055.

Saleh, T.A., 2020. Nanomaterials: Classification, properties, and environmental toxicities. Environmental Technology & Innovation, 20, p.101067.

Sannino, D., 2021. Types and Classification of Nanomaterials. Nanotechnology: Trends and Future Applications, pp.15-38.

Sarfraz, N. and Khan, I., 2021. Plasmonic gold nanoparticles (AuNPs): properties, synthesis and their advanced energy, environmental and biomedical applications. Chemistry–An Asian Journal, 16(7), pp.720-742.

Septembre-Malaterre, A., Lalarizo Rakoto, M., Marodon, C., Bedoui, Y., Nakab, J., Simon, E., Hoarau, L., Savriama, S., Strasberg, D., Guiraud, P. and Selambarom, J., 2020. Artemisia annua, a traditional plant brought to light. International journal of molecular sciences, 21(14), p.4986.

Shah, M.R., Ali, S., Ateeq, M., Perveen, S., Ahmed, S., Bertino, M.F. and Ali, M., 2014. Morphological analysis of the antimicrobial action of silver and gold nanoparticles stabilized with ceftriaxone on Escherichia coli using atomic force microscopy. New Journal of Chemistry, 38(11), pp.5633-5640.



Shakibaie, M., Forootanfar, H., Mollazadeh-Moghaddam, K., Bagherzadeh, Z., Nafissi-Varcheh, N., Shahverdi, A.R. and Faramarzi, M.A., 2010. Green synthesis of gold nanoparticles by the marine microalga Tetraselmis suecica. *Biotechnology and applied biochemistry*, *57*(2), pp.71-75.

Shapira, P. and Wang, J., 2009. From lab to market? Strategies and issues in the commercialization of nanotechnology in China. *Asian Business & Management*, *8*, pp.461-489.

Sharma, R., Garg, P., Kumar, P., Bhatia, S.K. and Kulshrestha, S., 2020. Microbial fermentation and its role in quality improvement of fermented foods. Fermentation, 6(4), p.106.

Sierra, J.A., Vanoni, C.R., Tumelero, M.A., Cid, C.C.P., Faccio, R., Franceschini, D.F., Creczynski-Pasa, T.B. and Pasa, A.A., 2016. Biogenic approaches using citrus extracts for the synthesis of

metal nanoparticles: the role of flavonoids in gold reduction and stabilization. New Journal of Chemistry, 40(2), pp.1420-1429.

Singer, A.C., Shaw, H., Rhodes, V. and Hart, A., 2016. Review of antimicrobial resistance in the environment and its relevance to environmental regulators. Frontiers in microbiology, 7, p.1728.

Singh, K.R., Nayak, V., Singh, J., Singh, A.K. and Singh, R.P., 2021. Potentialities of bioinspired metal and metal oxide nanoparticles in biomedical sciences. RSC advances, 11(40), pp.24722-24746.

Skirtach, A.G., Munoz Javier, A., Kreft, O., Köhler, K., Piera Alberola, A., Möhwald, H., Parak, W.J. and Sukhorukov, G.B., 2006. Laser-induced release of encapsulated materials inside living cells. *Angewandte Chemie International Edition*, *45*(28), pp.4612-4617.

Suganya, K.U., Govindaraju, K., Kumar, V.G., Dhas, T.S., Karthick, V., Singaravelu, G. and Elanchezhiyan, M., 2015. Blue green alga mediated synthesis of gold nanoparticles and its antibacterial efficacy against Gram positive organisms. Materials Science and Engineering: C, 47, pp.351-356.

Suschke, U., Sporer, F., Schneele, J., Geiss, H.K. and Reichling, J., 2007. Antibacterial and cytotoxic activity of Nepeta cataria L., N. cataria var. citriodora (Beck.) Balb. and Melissa officinalis L. essential oils. Natural Product Communications, 2(12), p.1934578X0700201218.

Tawfik, A., Nasr, M., Galal, A., El-Qelish, M., Yu, Z., Hassan, M.A., Salah, H.A., Hasanin, M.S., Meng, F., Bokhari, A. and Qyyum, M.A., 2021. Fermentation-based nanoparticle systems for sustainable conversion of black-liquor into biohydrogen. *Journal of Cleaner Production*, *309*, p.127349.

Tu, Y., 2011. The discovery of artemisinin (qinghaosu) and gifts from Chinese medicine. *Nature medicine*, *17*(10), pp.1217-1220.

Turkevich, J., Stevenson, P.C. and Hillier, J., 1951. A study of the nucleation and growth processes in the synthesis of colloidal gold. *Discussions of the Faraday Society*, *11*, pp.55-75.

Vilas, V., Philip, D. and Mathew, J., 2016. Biosynthesis of Au and Au/Ag alloy nanoparticles using Coleus aromaticus essential oil and evaluation of their catalytic, antibacterial and antiradical activities. Journal of Molecular Liquids, 221, pp.179-189.

Vollath, D., 2008. Nanomaterials an introduction to synthesis, properties and application. Environmental Engineering and Management Journal, 7(6), pp.865-870.

Willcox, M., 2009. Artemisia species: from traditional medicines to modern antimalarials—and back again. *The Journal of Alternative and Complementary Medicine*, *15*(2), pp.101-109.

Yadav, T. P., Yadav, R. M., and Singh, D. P. (2012). Mechanical milling: a top down approach for the synthesis of nanomaterials and nanocomposites. Nanosci. Nanotechnol. 2, 22–48. doi: 10.5923/j.nn.20120203.01

Yeo, W.W.Y., Maran, S., Kong, A.S.Y., Cheng, W.H., Lim, S.H.E., Loh, J.Y. and Lai, K.S., 2022. A Metal-Containing NP Approach to Treat Methicillin-Resistant Staphylococcus aureus (MRSA): Prospects and Challenges. Materials, 15(17), p.5802.

Yulo, P.R.J. and Hendrickson, H.L., 2019. The evolution of spherical cell shape; progress and perspective. Biochemical Society Transactions, 47(6), pp.1621-1634.

Zeb, S., Ali, A., Zaman, W., Zeb, S., Ali, S., Ullah, F. and Shakoor, A., 2018. Pharmacology, taxonomy and phytochemistry of the genus Artemisia specifically from Pakistan: a comprehensive review. Pharmaceutical and Biomedical Research, 4(4), pp.1-12.

Zhang, B., Misak, H., Dhanasekaran, P.S., Kalla, D. and Asmatulu, R., 2011, September. Environmental impacts of nanotechnology and its products. In Proceedings of the 2011 Midwest Section Conference of the American Society for Engineering Education (pp. 1-9).

Zhang, Y., Shareena Dasari, T.P., Deng, H. and Yu, H., 2015. Antimicrobial activity of gold nanoparticles and ionic gold. Journal of Environmental Science and Health, Part C, 33(3), pp.286-327.

Zsigmondy, R., 1909. *Colloids and the ultramicroscope: a manual of colloid chemistry and ultramicroscopy*. J. Wiley & sons.

# Chapter 2: Materials and Methods

## 2.1. Materials

All chemicals used in this project were used without further purification. The Gold (III) chloride hydrate ($HAuCl_4 \bullet XH_2O$) precursor with 99.93 % purity was obtained from LeapChem Co., Ltd, Hangzhou, China. The ultra-pure water used was obtained from the Department of Chemistry, University of *the* Western Cape, Bellville, South Africa. The *Artemisia annua* plant extract was supplied from Prof Vincent Omolo, Masinde Muliro University of Science and Technology, Kenya in powder form and stored in a sterile glass vial.

The assessment of the antimicrobial activity of *A.annua* and the synthesized *A.annua*-AuNPs was carried out using 6 different bacterial strains shown in Table 2.1 and Ciprofloxacin (Sigma Aldrich, Schnelldorf) as a positive control.

Table 2.1**:** Bacterial strains used and their gram stain

| Cell line | Abbreviations | Cell type | ATCC No. | Gram stain |
|---|---|---|---|---|
| *Escherichia coli* | *E.coli* | Bacterial | ATCC 35281 | Negative |
| *Klebsiella pneumoniae* | *K.pneumoniae* | Bacterial | ATCC 13883 | Negative |
| *Methicillin-resistant Staphylococcus aureus* | *MRSA* | Bacterial | ATCC 33591 | Positive |
| *Pseudomonas aeruginosa* | *P.aeruginosa* | Bacterial | ATCC 27853 | Negative |
| *Staphylococcus aureus* | *S.aureus* | Bacterial | ATCC 25923 | Positive |
| *Staphylococcus epidermidis* | *S.epidermidis* | Bacterial | ATCC 12228 | Positive |

All the microorganisms used were obtained from the Biolabels laboratory, University of *the* Western Cape, Bellville, South Africa.

Table 2.2: List of equipment and suppliers.

| Equipment | Supplier |
|---|---|
| FEI Tecnai G2 F20 field-emission gun | Field Electron and Ion Company, Hillsboro, USA |
| Hot plate & magentic stirrer | FMH instruments, RSA |
| Incubator Vortemp 1550 | Labnet International, Edison, USA |
| Mini spin plus centrifuge | Epperndorf Centrifuge |
| POLARstar Omega multi-detection microplate reader spectrometer | BMG LABTECH, Germany |
| Thermo Nico-let 6700 | Thermo Fisher Scientific, U.S |
| Zetasizer Nano-ZS90 instrument | Malvern Panalytical Ltd, UK |

## 2.2. Methods

### 2.2.1. Preparation of *Artemisia annua* aqueous extract

The *Artemisia annua* aqueous extract was prepared at a concentration of 50 mg/mL. Briefly, 2.5 g of fine powder was added to a 100 mL Erlenmeyer flask containing 50 mL of ultra-pure water. The mixture was boiled for 15 minutes with constant magnetic stirring and allowed to cool at room temperature. The vacuum filtration method was then used to filter the resulting brown aqueous extract using a Buchner funnel and grade 1 Whatman filter papers of 125 mm diameter. The filtrate was used for the reduction of the precursor to form AuNPs and was stored in a dry cool place for later use. The extract solution was freshly prepared whenever there are signs of mold and turbidity.

### 2.2.2. Synthesis of *A.annua*-AuNPs

The phytochemical synthesis of *A.annua*-AuNPs was done by using the following procedure. Briefly, 1mM of $HAuCl_4 \bullet XH_2O$ standard solution was prepared into a 50 mL volumetric flask. Using a measuring cylinder, 45 mL was withdrawn from the $HAuCl_4 \bullet XH_2O$ standard solution and mixed with 5 mL *Artemisia annua* aqueous extract of known concentration in a 50 mL plastic centrifuge tube. The tube was incubated using Vortemp 1550 (Labnet International, Edison, USA) at 25 °C, 500 rpm for 1 hour. The color change from yellow to wine-red color confirmed the success of the synthesis of AuNPs.

### 2.2.3. Stability testing of *A.annua*-AuNPs

The stability of the *A.annua*-AuNPs in biological media was evaluated in Mycorrhiza helper bacteria (MHB) and Luria-Bertani (LB) broth. This assay was performed immediately after the *A.annua*-AuNPs were purified. In glass test tubes, 250 µL of aqueous solutions of *A.annua*-AuNPs were mixed with the same volume of the media. The tubes were incubated at 25 °C or 37 °C for 24 h. The stability of these nanoparticles was evaluated by monitoring UV-Vis spectra.



## 2.3. Optimisation study

To optimize the phytochemical synthesis of *A.annua*-AuNPs, the effect of reaction conditions such as *Artemisia annua* extract, $HAuCl_4 \bullet XH_2O$ concentrations, and incubation time was varied. Furthermore, different pH and temperature were also optimized by monitoring UV-VIS and analyzing the surface resonance peak (SPR).

## 2.4. Characterisation of *A.annua*-AuNPs

The AuNPs were synthesized on a large scale using the optimized conditions and were characterized using the following techniques.

### 2.4.1. UV-VIS spectroscopy

The UV–VIS spectroscopy was done on POLARstar Omega multi-detection microplate reader spectrophotometer (BMG Labtech, Germany) at room temperature to confirm the formation of *A.annua*-AuNPs at wavelengths range 400–900 nm.

UV-Vis spectroscopy is a technique that works based on the measurement of the attenuation of electromagnetic radiations when passing through matter at a specific wavelength. The working principle of UV-Vis is based on the phenomenon of electronic excitation. When UV radiation is passed through the sample, the atoms or molecules absorb the energy and move from the ground state to the excited state. The amount of radiation absorbed by the analyte is then measured as a function of wavelength producing a spectrum.

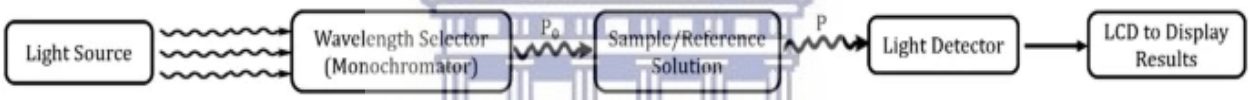


Figure 2.1: The schematic diagram showing the basic components of the UV-Vis spectroscopy instrumentation (Akash and Rehman., 2020).



The light source is the basic requirement and the commonly used type is a deuterium lamp for radiation at UV region (200-400 nm) and tungsten halogen lamps for producing visible region radiation (400-750 nm). The light source is responsible for passing the polychromatic radiation to the monochromator. The monochromators such as filters, prisms, and/or gratings then convert the wide band of polychromatic light radiation into a narrow band of monochromatic radiation which results in the light of only a single wavelength being passed into the sample holder containing the analyte. Cuvette made up of quartz is used as a sample holder and it allows the light passing through the analyte to be sent to the detector where it gets detected and amplified. The detector such as the photomultiplier tube converts the light energy into an electrical signal which is then sent into the recorder. The recorder displays the electric signal in form of the form of a graph (Akash and Rehman., 2020).

### 2.4.2. FTIR spectroscopy analysis

Fourier transforms infrared (FTIR) spectrometry was performed on a Nico-let 6700 (Thermo Fischer, US) in a range of 400–4000 $cm^1$ to analyze the possible functional group present in *A.annua* extract and *A.annua*-AuNPs. The sample was prepared by first centrifuging 2 mL of each sample at 8000 rpm for 15 minutes using Mini-spin plus instrument (Eppendorf Centrifuge). The pellets were washed 3 times and dried. The resulting dried powder was grounded with KBr using pistil and mortar. Lastly, the FTIR pellet was created using a KBr pellet hand press.

FTIR spectroscopy studies the interaction of the infrared region of the electromagnetic spectrum with that of matter. The working principle of FTIR spectroscopy involves the passing of infrared light through the sample material. Depending on the energy levels, this light can trigger the vibrations of specific molecular bonds (absorption). The most prominent molecular vibrations are stretching vibrations (symmetric, and antisymmetric stretching vibrations), and bending vibrations (in-plane, and out-plane bending vibrations). The energy absorbed by the molecule is consumed causing a decrease in the original IR beam.

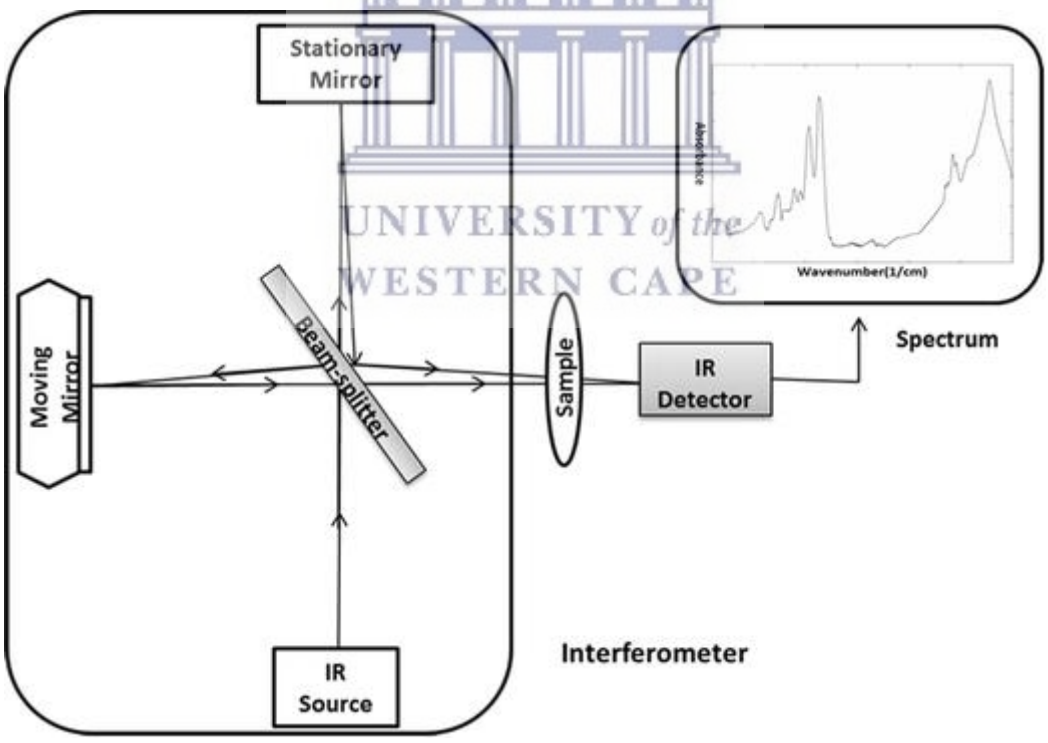


Figure 2.2: The schematic diagram of the FTIR spectroscopy (Faghihzadeh et al., 2016)

IR radiation is continuously generated by a light source such as Globar which is made up of silicon carbide (SiC). The SiC is heated electronically generating a continuous IR radiation that is then directed into the sample cell. The Quartz halogen lamp, a high-pressure mercury discharge lamp, and a laser are other types of IR radiation sources that are commonly used. The sample cell holds the analyte and it allows the monochromatic light to pass through it. Depending on the form of the analyte, different sample cells are used. The alkali halides such as KBr are used when analyzing solids and aqueous analytes could be dropped in the sample compartment of the instrument provided that it can analyze them. The FTIR spectrometer containing the interferometer directs the IR beam into the beam splitter which separates the beam into two separate beams that are directed at the fixed and the moving mirror respectively. Then the light travels back into a beam splitter where it is recombined causing the interference and is then directed into the sample material. This allows the simultaneous reading of spectral information of all wavelengths which are detected and amplified by the IR detector. The IR detector produces the raw signal of light intensity versus the mirror position. To obtain a sample spectrum, the background noise is removed by measuring a spectrum of the sample cell (KBr) without the presence of the sample. This raw signal is mathematically Fourier transformed into the classical IR spectrum of light intensity versus wavenumbers. The sample is then inserted and the sample spectrum is generated. The sample spectrum is then divided by the reference spectrum which yields the final classic view of the FTIR transmission spectrum. The generated spectrum acts like a "chemical fingerprint" which allows the identification of unknown samples and the characterization of materials (Akash and Rehman., 2020).



### 2.4.3. DLS analysis

The DLS analysis was used to determine particle size distribution, polydispersity index (PDI), and zeta potential, and it was performed on Zetasizer Nano ZS90 (Malvern, UK).

Dynamic light scattering spectroscopy measures the Brownian motion of particles in dispersion and uses the information to determine their hydrodynamic size. The Brownian motion is defined as the random movement of particles that are caused by their collision with solvent molecules such as water. It uses the basic that smaller particles move or diffuse faster than larger particles. The rate of Brownian motion is quantified as a translational diffusion coefficient (D). The hydrodynamic size measured is defined as a sphere that diffuses at the same rate as the particle being measured. This sphere is made up of a core particle and the ions or adsorbed polymers on its surface.

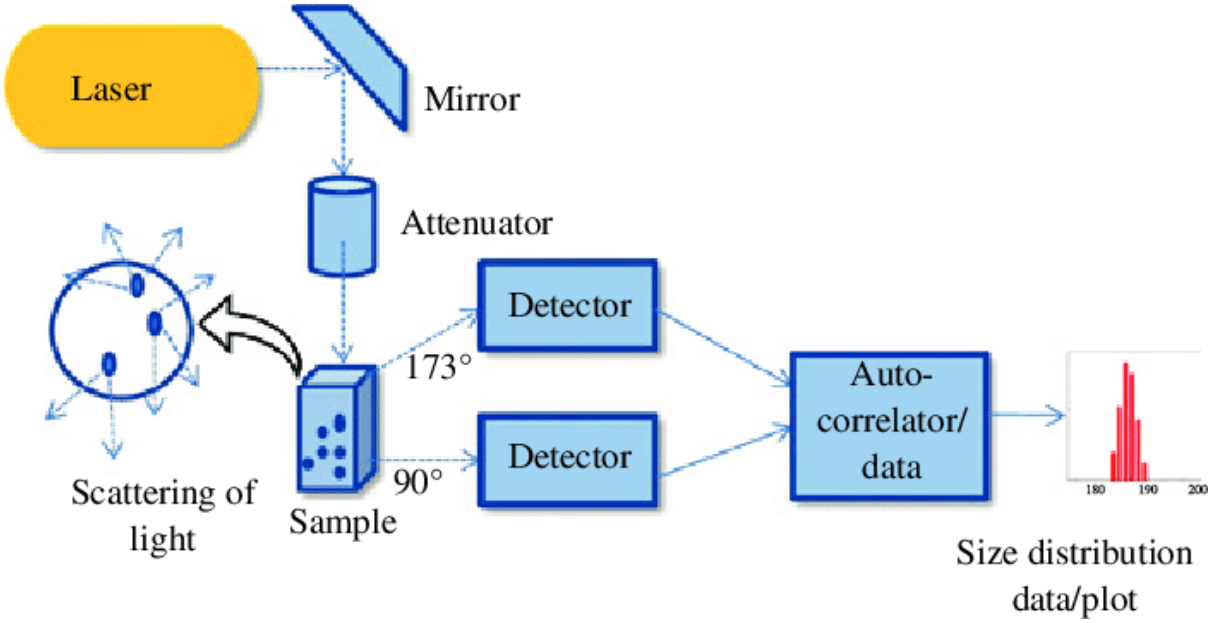


Figure 2.3: The schematic diagram showing the instrumentation of DLS (Mahmood et al., 2017).

The diffusion rate is measured when the laser illuminates some of the particles in the sample causing the scattering of some of the light that hits them. If the particles were still, they would measure a completely constant intensity of scattered light. However, in the dispersion sample, the diffusion causes the intensity of light scattered by the particles to fluctuate over time. The scattering of this light from many randomly diffusing particles is sent to the detector where it is combined to create a fluctuating intensity signal over time. The auto-correlator then creates the data of size distribution by using the basis that the larger the particles being measured the more slowly they diffuse and the longer it takes for the complete loss of correlation. On the other hand, smaller particles have a rapid diffusion causing a rapid correlation of the signal. The auto-correlation provides the translational diffusion coefficient (D) which the instrument uses the mathematical Stokes-Einstein equation to provide the hydrodynamic size of the sample (Babick., 2020).

### 2.4.4. HRTEM analysis

The examination of the particle size and morphology was carried out on an FEI Tecnai G2 F20 field-emission gun (Field Electron and Ion Company, Hillsboro, USA) at 200 kV. EDX and the SAED were also obtained from HRTEM. For the preparation for HR-TEM, a drop of *A.annua*-AuNPs solution was loaded onto a carbon-coated copper grid. The grid was dried under a Xenon lamp for 10 min before analysis. The TEM micrographs were analyzed using Image J Software for size distribution.

High-resolution transmission electron microscopy (HRTEM) is the TEM imaging mode that provides images of the atomic structure of the sample. It allows the imaging of the crystallographic patterns of the material hence providing crystalline information about the sample.

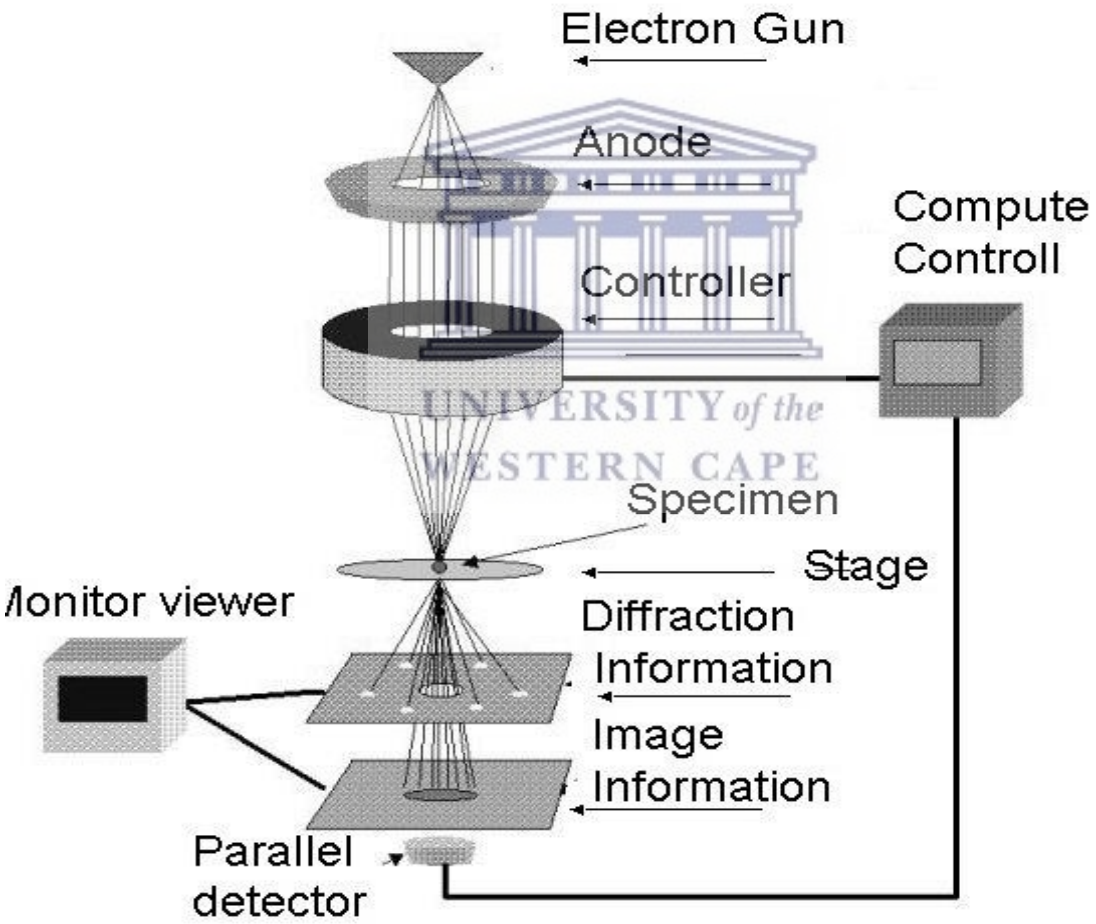


Figure 2.4: The schematic diagram of HRTEM (Baruwati., 2007)

The electron gun produces the electron beam which is the cathode in the form of the heated tungsten filament. The electrons emitted are accelerated toward the sample with the help of the anode. The anode then allows the electrons to pass through the aperture. The condenser system contains the condenser lens/magnetic lens which condenses the electron beam hence focusing the electron beam into the sample/specimen. The intensity and angular aperture of the beam are controlled by the condenser lens system which is kept between the anode and the specimen. The image-producing system consists of objective and intermediate lenses which focus the electrons passing through the specimen to form a real and highly magnified image. The objective length is used for the short focal length (1-5 mm) and produces a real intermediate image. The intermediate image is then amplified and magnified with the help of the projector lens. The image is finally obtained in the fluorescence screen. The final component is the image recording system which converts the electron image into the format that can be seen on the monitor. The HRTEM generally provides a two-dimensional image (2D) (Ernst and Rühle., 1997).

### 2.5. Antimicrobial activity study

The antimicrobial activity of *A.annua* extract and *A.annua*-AuNP against six different bacterial strains was evaluated by determining their MIC using a microdilution assay. A total of 3 Gram-positive strains, *S. aureus* (ATCC 25923), *S. epidermidis* (ATCC 12228), and MRSA (ATCC 33591) were used, with a total of 3 Gram-negative strains *K. pneumoniae* (ATCC 13883), *E. coli* (ATCC 35281), and *P. aeruginosa* (ATCC 27853). Briefly, 50 µL of *A.annua*-AuNPs (in MHB) were added in 96-well plates with decreasing concentrations (320, 160, 80, 40, 20, 10, 5, and 2.5 µg/mL). Microbial suspensions of the bacteria were cultured in MHB and diluted until they reached a 0.5 McFarland standard (standard is approximately 1 × 108 CFU/mL). A volume of 50 µL of the microbial suspensions was added to each well containing MHB and AuNPs. The plates were sealed and incubated for 24 h at 37 °C. Ciprofloxacin (2.5 mg/mL) was used as the positive control for the bacteria, while sterile deionized water was used as the negative control. After incubation, 10 µL of Alamar Blue was added to each well and the plate was incubated for 3 h in the dark. In the presence of viable bacteria, the non-fluorescent Alamar Blue dye (resazurin) was reduced to resofurin, a pink compound that was highly fluorescent. Therefore, the intensity of the pink color and the fluorescence was proportional to the number of viable cells present. The MIC was then determined using a spectrophotometer at a

fluorescence excitation/emission wavelength of 530–560/590 nm. The screening was performed in triplicates.

**References**


Akash, M.S.H. and Rehman, K., 2020. Ultraviolet-visible (UV-VIS) spectroscopy. In *Essentials of Pharmaceutical Analysis* (pp. 29-56). Springer, Singapore.

Babick, F., 2020. Dynamic light scattering (DLS). In Characterization of Nanoparticles (pp. 137-172). Elsevier.

Baruwati, B., 2007. Studies on the synthesis, characterization, surface modification and application of nanocrystalline nickel ferrite. *India Institute of Chemical Technology Hyderabad*.

Ernst, F. and Rühle, M., 1997. Present developments in high-resolution transmission electron microscopy. Current Opinion in Solid State and Materials Science, 2(4), pp.469-476.

Faghihzadeh, F., Anaya, N.M., Schifman, L.A. and Oyanedel-Craver, V., 2016. Fourier transform infrared spectroscopy to assess molecular-level changes in microorganisms exposed to nanoparticles. *Nanotechnology for environmental engineering*, *1*(1), pp.1-16.

Mahmood, S., Mandal, U.K., Chatterjee, B. and Taher, M., 2017. Advanced characterizations of nanoparticles for drug delivery: investigating their properties through the techniques used in their evaluations. *Nanotechnology Reviews*, *6*(4), pp.355-372.

# Chapter 3: Results and Discussion

## 3.1. Synthesis of *A.annua*-AuNPs

Generally, AuNPs are synthesized by the reduction of gold chloride ($HAuCl_4 \bullet XH_2O$) solution into gold ions ($Au^{3+}$ to $Au^0$) (Akintelu et al., 2021). The chemical synthesis was previously been widely used for the synthesis of stable metallic nanoparticles such as AuNPs. The common methods of the chemical synthesis of nanoparticles amongst many include co-precipitation, Sol-gel method, microwave, hydrothermal synthesis, etc.

The major two basic requirements for chemical synthesis are:

- the presence of reducing agents such as borohydrides, hydrogen peroxides, sulfites, and many others. These chemical compounds are responsible for providing the electrons to reduce the gold ions auric ($Au^{3+}$) and aurous ($Au^+$) into $Au^0$ which is the oxidation state for gold nanoparticles (Souza et al., 2019).
- the presence of stabilizing agents such as phosphorus and sulfur ligands, polymers, surfactants, and others. Due to the tendency of aggregation of nanoparticles in colloidal solutions, these agents bring stability by causing a repulsive force that controls the final size, shape, the rate of nanoparticles growth. The stabilizing agent may also act as a stabilizing agent.

The chemical method is associated with many adverse effects due to the presence of some toxic chemicals absorbed on the surface of the nanoparticles (Hasan., 2015). The green synthesis method of AuNPs using plant extracts was then found to be a solution to eliminate the use of toxic solvents. Plant extracts contain phytochemicals such as polyphenols, terpenoids, and saponins that are responsible for the reduction of gold salt (Basavegowda et al., 2014). Geethalakshmi and Sarada have synthesized the AuNPs and AgNPs using the saponin-rich extract of *Trianthema decandra.* The saponin extract was obtained by adding methanol into the water extract of the *T.decandra* which was followed by the fractionation of the precipitated insoluble portion on a silica gel column. The saponin-rich extract was used to reduce $HAuCl_4$ and $AgNO_3$ respectively without the use of a capping agent. They synthesized AuNPs with a variety of shapes such as hexagons, cubic, and spheres, whereas AgNPs had spherical shapes only (Geethalakshmi and Sarada., 2013). On the other hand, Huang and co-workers have used a one-step synthesis of AuNPs at room temperature using Bayberry tannin (BT). There were no additional reagents or treatments used. They obtained BT-AuNPs that are sized controllable

with a particle size of 1.8 ± 0.3 nm when using a BT concentration of 800 mg (Huang et al., 2010).

It is a known fact that the composition and amount the phytochemicals vary from plant to plant depending on the geographic variation, soil properties, and climate. Fu and co-authors have evaluated 23 batches of *Artemisia annua* collected in 12 different provinces of China. The quality of *A.annua* was evaluated by using High-performance liquid chromatography with photodiode-array detection (HPLC-DAD) where 5 flavonoids, 2 coumarins, and 4 sesquiterpenes were simultaneously quantified. The High-performance liquid chromatography coupled with electrospray ionization-quadrupole-time of flight-mass spectrometry (LC-ESI-QTOF-MS/MS) was used to avoid obtaining false positive results. The results showed high artemisinin and isorhamnetin contents across the south of the Yangtze River whereas in eastern and northern China the high contents of scopolin, scopoletin, chrysosplenol D, casticin, arteannuin B, and artemisinic acid were obtained (Fu et al., 2020). Furthermore, Safari and colleagues have evaluated the effect that the climate and soil property has on essential oil components of *Ferulago angulate*. They collected the aerial parts of the plant from different elevations (2500, 3000, and 3500 m above sea level) and three different regions mostly mountains named Kallar, Mili, and Saldaran mountains of southwest Iran. The Clevenger apparatus was used to estimate the essential oil content with phytochemicals being assayed using gas chromatography/mass spectrometry (GC / MS). The results showed the most alpha-phinene, betaocimene, and cis-ocimene on Saldaran mountain at 3000 m elevation. The phytochemicals such as α-thujene, α-phellandrene, and nonadecane were found abundant in Kallar mountain which has a clay loam soil texture. The sandy soil clay soil of Milli Mountain at 3500 m elevation showed the lowest levels of these nutrients (Safari et al., 2019).



Because of these factors that affect the phytochemical content of plants, there is a need to optimize the green synthesis of AuNPs using *Artemisia annua* plant extract. As such this quantity of UV-Vis spectra demonstrates polydispersity of the obtained AuNPs. See UV-Vis spectra sections 3.2.1 to section 3.3.1. This is further confirmed by results obtained from HRTEM analysis section 3.3.4. The success in the synthesis of *A.annua*-AuNPs was indicated by a color change of the solution (*Artemisia annua* plant extract and $HAuCl_4 \bullet XH_2O$) from yellow to ruby-red. The ruby red color of the synthesized *A.annua*-AuNPs is supported by Das and associates who synthesized gold nanoparticles using an ethanolic flower extract of *Nyctanthes arbortristis* plant. The extract was allowed to react with $HAuCl_4$ aqueous solution for 30 minutes at a temperature of 80 ºC. They observed the color change from the original

yellow to shades of red within 30 minutes which they claim confirms the visual success in the formation of AuNPs (Das et al., 2011). The ruby-red color of the gold nanoparticle was also observed by Islam and colleagues when *Pistacia integerrima* gall extract was used to reduce $HAuCl_4$ aqueous solution into AuNPs (Islam et al., 2019). Furthermore, the AuNPs synthesized using *Ananas comosus* as a reducing agent which was added into $HAuCl_4$ (6 mM) and reacted for 6 hours were reported to produce a dark ruby red color (Bindhu and Umadevi., 2014). During the synthesis of the *A.annua*-AuNPs, the addition of the plant extract into the $HAuCl_4 \bullet XH_2O$ solution resulted in no change in color (Figure 3.1.1. A). As the reaction time increases close to 1 hour, the color of the solution changed to ruby-red of high intensity (Figure 3.1.1. B).

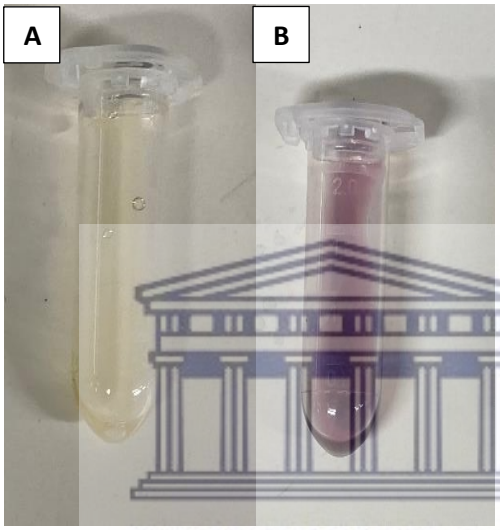




Figure 3.1.1: The color change of A.annua-AuNPs (A) 0 min and (B) after 1 hour incubation time at a temperature of 25 ºC.

This observation in a color change of the reaction mixture was attributed to the surface plasmon resonance (SPR) caused by the collective oscillations of free conduction electrons that are induced by their interaction with the electromagnetic field (Figure 3.1.2.) (Suman et al., 2014).

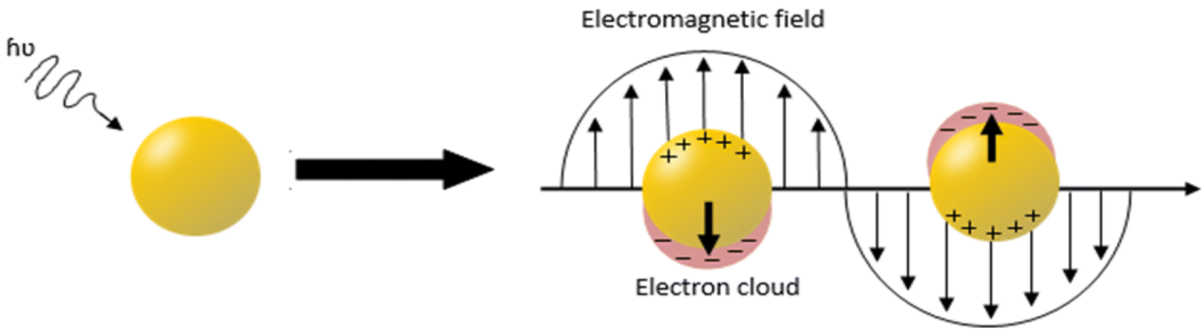

Figure 3.1.2: A schematic diagram of the oscillation of the free electrons of the nanoparticle (Fuller and Köper., 2019)

AuNPs are well known to exhibit a ruby-red color that depends on the position of the surface plasmon resonance (SPR) peak on the electromagnetic spectrum which is determined by the shape and size of the nanoparticles (Madhusudhan et al., 2019). UV-VIS spectroscopy is a very useful technique that has been previously used to confirm the synthesis and stability of AuNPs (ElMitwalli et al., 2020); Asnag et al., 2019). Dubey and colleagues have used UV-Vis spectroscopy to confirm the success in the synthesis of gold nanoparticles from the reduction of 1mM auric acid using leaves extracts of *Rosa rugosa*. They obtained a characteristic SPR band around 578 nm (Dubey et al., 2010). AuNPs also exhibit a variety of colors such as red to purple (Figure 3.1.3). To illustrate the effect that the size of the nanoparticle has on the position of the SPR, a study done by Subara and Jaswir has reported on spherical AuNPs of different sizes with a minimum diameter of 13 nm having a $\lambda_{max}$ appearing around 520 nm while 99 nm AuNPs absorbs around 600 nm wavelength of the UV-Vis spectrum. Moreover, it is also evident that an increase in the size of the spherical nanoparticles results in the shift of the SPR peak to the larger wavelength values of the electromagnetic spectrum (red-shift) (Subara and Jaswir., 2018).

.

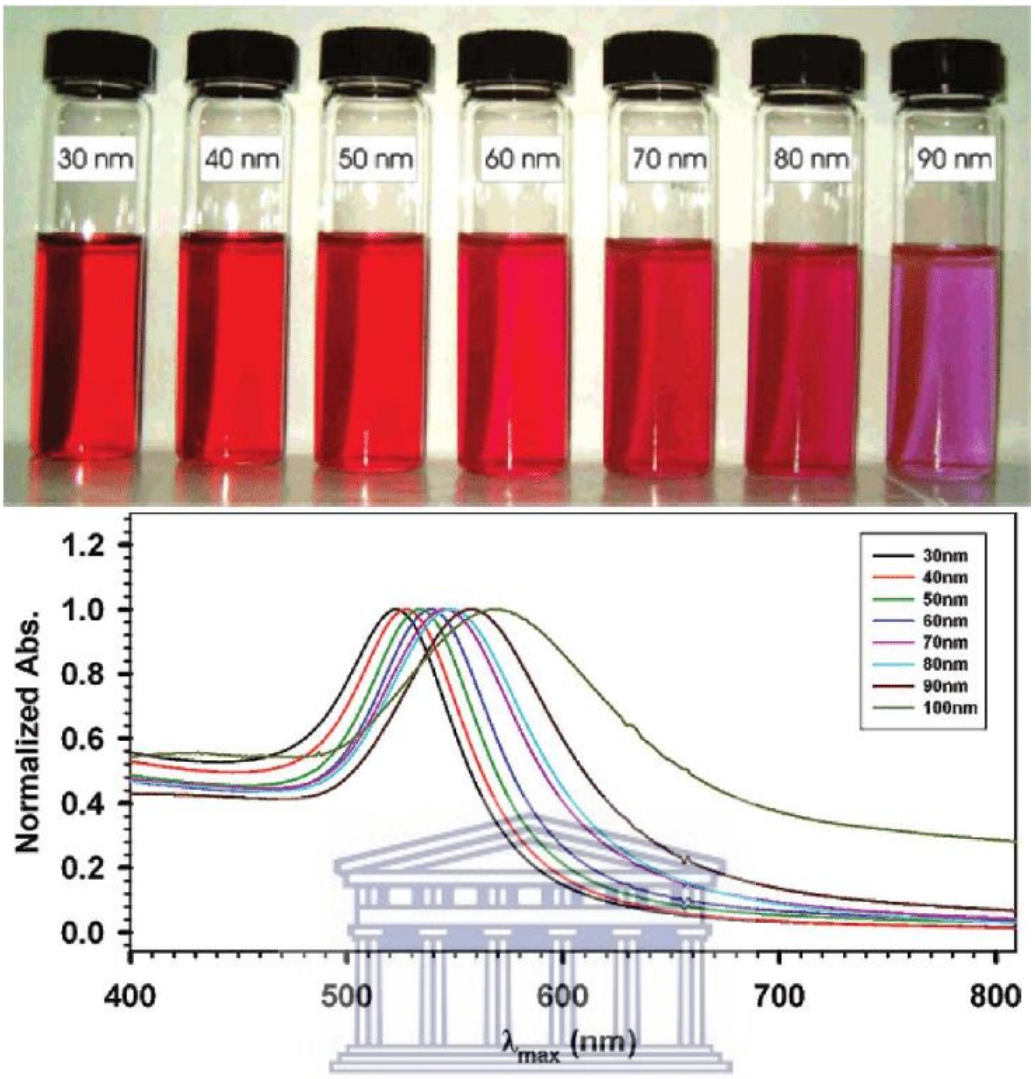


Figure 3.1.3: Different colors of AuNPs having different particle sizes (Subara and Jaswir., 2018)



The maximum absorbance ($\lambda_{max}$) for the synthesized *A.annua*-AuNPs appeared at 550 nm which is characteristic of AuNPs (Basavegowda et al., 2014). These results are supported by the study done by Prema and co-workers. They synthesized gold nanoparticles using the extract from *Camellia sinensis* L. (green tea) as a reducing agent of $HAuCl_4 \cdot 3H_2O$ solution to investigate a potential antiproliferative effect. The UV-Vis spectroscopy has shown an SPR peak around 540 nm wavelength which supports the 550 nm value of the synthesized *A.annua*-AuNPs (Prema et al., 2022). Although AuNPs are among the most studied nanoparticles, there has been a challenge of the plausible mechanism not fully understood which raises health concerns (Acharya et al., 2019). A study by Olga and associates reported the toxicity (on

environment and ecosystems), system mechanism, nanoparticle waste management, and the assessment of the sustainability of the green synthesis as major concerns (Olga et al., 2022).

### 3.2. Optimisation study

To optimize the biosynthesis of *A.annua*-AuNPs, the effect of reaction conditions such as incubation time, pH, gold salt, and plant extract concentrations were varied. In this technique, the reaction variables were varied while others were held constant. Satpathy and colleagues have used this method to synthesize gold nanoparticles using *Hygrophila spinosa* aqueous extract. They synthesized AuNPs by reducing the $HAuCl_4 \cdot 3H_2O$ with *H. spinosa* aqueous extract. Various concentrations of $HAuCl_4 \cdot 3H_2O$ (1, 2, 4, 6, and 8 mM) were varied as well as that of *H. spinosa* aqueous extract (10, 30, 50, 70, and 90% v/v). Different reaction parameters such as temperature were also varied from room temperature to 100 °C. Further parameters such as reaction time (15, 30, 45, and 60 min) and pH of the reaction mixture were also varied (2, 4, 6, 8, and 12) using sodium hydroxide or hydrochloric acid (Satpathy et al., 2020).

#### 3.2.1. The Effect of $HAuCl_4 \cdot XH_2O$ concentration on the synthesis of *A.annua*-AuNPs.

The effect of gold (III) chloride was investigated by preparing 6 different concentrations (0.25 - 10 mM). The formation of *A.annua*-AuNPs was monitored by analyzing the surface plasmon resonance (SPR) using UV-VIS on a wavelength region from 400-900 nm. The effect of $HAuCl_4 \cdot XH_2O$ concentration on the synthesis of *A.annua*-AuNPs is represented by Figure 3.2.1.

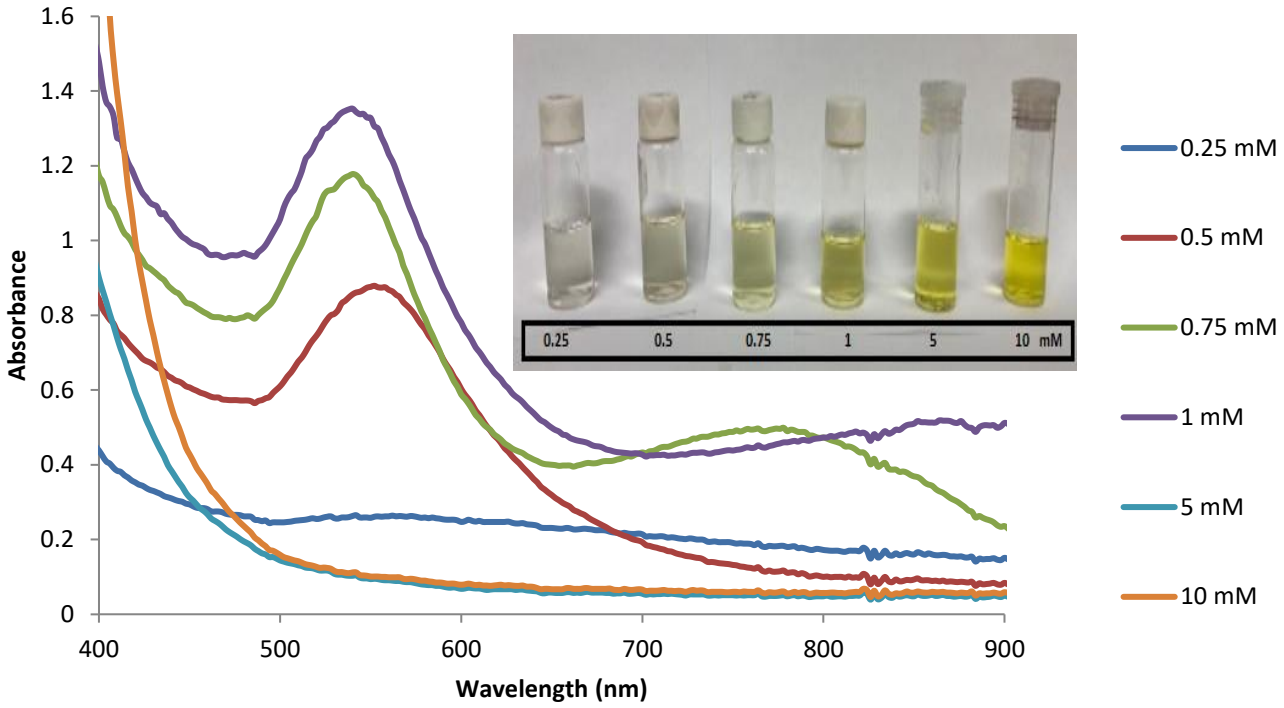


Figure 3.2.1: A UV-VIS spectra of the biosynthesized gold nanoparticles using 50 mg/ml *Artemisia annua* extract concentration, 25 ºC, 500 RPM, 1hr incubation time, and different $HAuCl_4$ concentrations.



The use of 1 mM $HAuCl_4 \bullet XH_2O$ concentration produced AuNPs with the highest SPR peak. Moreover, 1 mM $HAuCl_4 \bullet XH_2O$ has produced a larger quantity of AuNPs which is shown by its height being the highest than other concentrations. It has been reported that the height of the absorbance peak is directly proportional to the concentration of AuNPs in a solution (Elbagory et al., 2016). This fact is supported by Tyavambiza and colleagues who synthesized silver nanoparticles by reducing silver nitrate using an extract from *Cotyledon orbiculate.* The effect of silver nitrate concentration was investigated using two concentrations (1 and 3 mM). It was concluded that the concentration of 3 mM produced a large amount of AgNPs which is shown by the height of the absorbance peak (Tyavambiza et al., 2021). Furthermore, a 1 mM concentration has been commonly reported for the synthesis of AuNPs. Gürsoy and colleagues have used a green synthesis method to synthesize gold nanoparticles for antifungal activity. The AuNPs were synthesized by using the aqueous extract of green algae (*Chlorella sorokiniana*) as a reducing agent of $HAuCl_4$. Upon optimization of the reaction conditions, they find the optimum condition for their synthesis to be 1mM $HAuCl_4$ concentration, pH value of 6, and 60-minute incubation time (Gürsoy et al., 2021). The 1 mM concentration of $HAuCl_4$ was also reported by Fadaka and associates where they synthesized AuNPs using the leaf

extract of *Pimenta dioica* to reduce the $HAuCl_4$ solution (Fadaka et al., 2021). Further use of a 1 mM concentration of $HAuCl_4$ was observed in the synthesis of gold nanoparticles using banana pith extract as a reducing agent (Nayak et al., 2021). Figure 3.2.1. shows the 0.75 mM $HAuCl_4 \bullet XH_2O$, has produced two SPR bands, one between 500-600 nm and the other from 700-900 nm. This shows the presence of rod-shaped AuNPs (Shajari et al., 2017). The $\lambda_{max}$ shift to higher values is observed on 0.5 mM which is a redshift, a phenomenon where nanoparticles produced have an increase in size which is not suitable for antimicrobial application (Elbagory et al., 2016). Consequently, the optimum concentration of $HAuCl_4 \bullet XH_2O$ solution for the synthesis of *A.annua*-AuNPs was found to be 1 mM. Deepak and colleagues support the success in the synthesis of AuNPs when using a 1 mM concentration of HAuCl4 (Deepak et al., 2011). The purified URAK was used as a reducing agent and their results show the absorbance peak of AuNPs at 450 nm incubated for 60 hours whereas our *A.annua*-AuNPs absorbs around 540 nm using 1 hour incubation time.

### 3.2.2. Effect of *A.annua* aqueous extract concentration and temperature on the synthesis of *A.annua*-AuNPs.

The temperature was another parameter evaluated during the synthesis of *A.annua*-AuNPs. Generally, an increase in temperature is associated with an increase in reaction rate which favors the synthesis of nanoparticles (Tyavambiza et al., 2021). This fact is supported by the collision theory of particles which states that particles only react when they collide with each other. Heating the particle supply them with sufficient energy causing them to move faster hence resulting in an effective collision. These collisions are of high energy that overcomes the activation energy of the reaction and increases the rate of the reaction (Burton., 2013). As the temperature increased from 50 to 70 °C (Figure 3.2.2 B and C), the absorption peaks became broad and lowered. This demonstrates a decrease in the number of nanoparticles produced at higher temperatures. Furthermore, the reaction temperature of 100 °C did not produce any nanoparticles hence for the synthesis of *A.annua*-AuNPs, 25 °C was used as the optimum temperature (OT). Plant extract concentration is another reaction parameter that was evaluated. A total of 7 *A.annua* plant extract concentrations (1.56 – 100 mg/mL) were tested and only three concentrations (100, 50, and 25 mg/mL) formed *A.annua*-AuNPs at 25 °C (Figure 3.2.2-A). This shows that the lowest plant extract concentrations hindered the formation of *A.annua*-AuNPs. It is evident in Figure that 50 mg/mL plant extract concentration at 25 °C has the

highest absorbance than 100 mg/mL. This suggests that more nanoparticles were produced. Moreover, 100 mg/mL is red-shifted which shows an increase in the size of *A.annua*-AuNPs. Hence for the synthesis of A.annua-AuNPs, a plant concentration of 50 mg/mL and temperature of 25 °C was used. The temperature of phytochemical synthesis of nanoparticles has been associated to affect the size, shape, and amount of nanoparticles produced. A study by Elbergory and colleagues synthesized a variety of AuNPs using 17 South African plants (Elbagory et al., 2016). The incubation temperature of 25 °C was used and their study reported that lower temperatures are associated with larger nanoparticle sizes and a variety of shapes which supports the findings of this study.

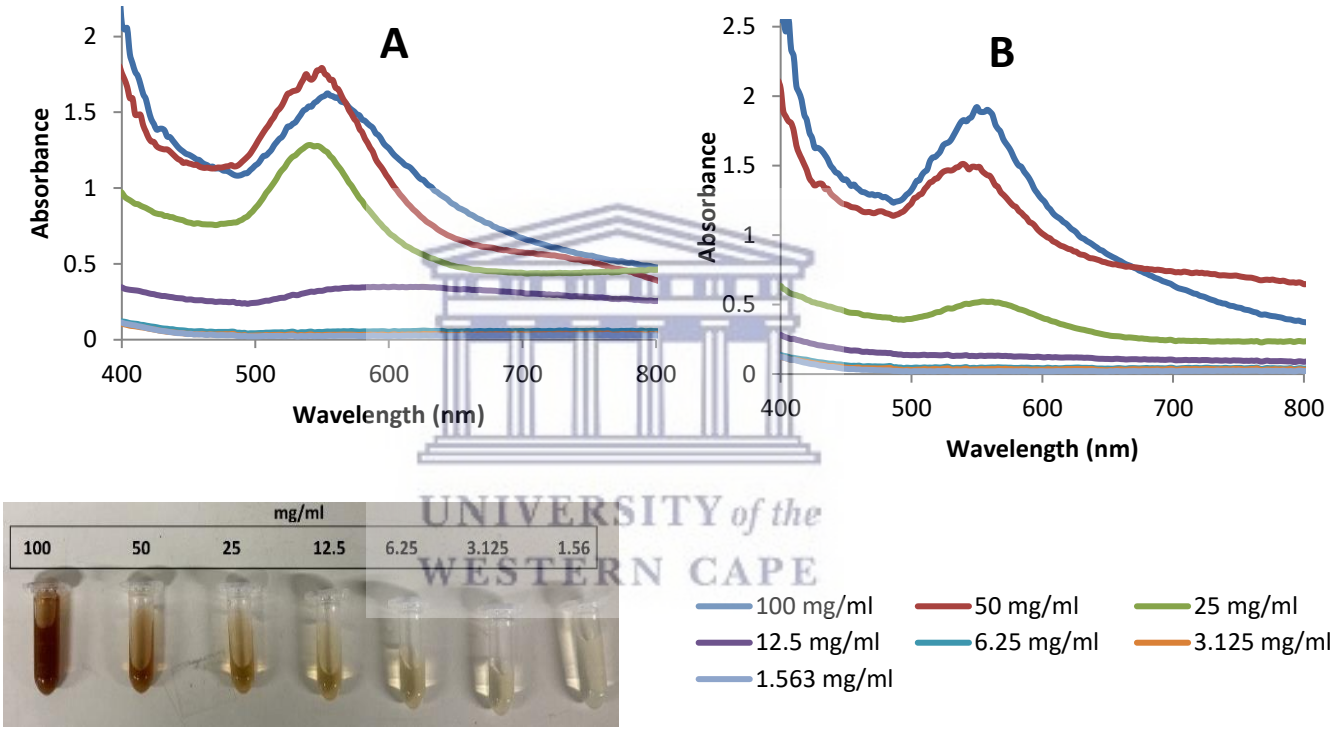

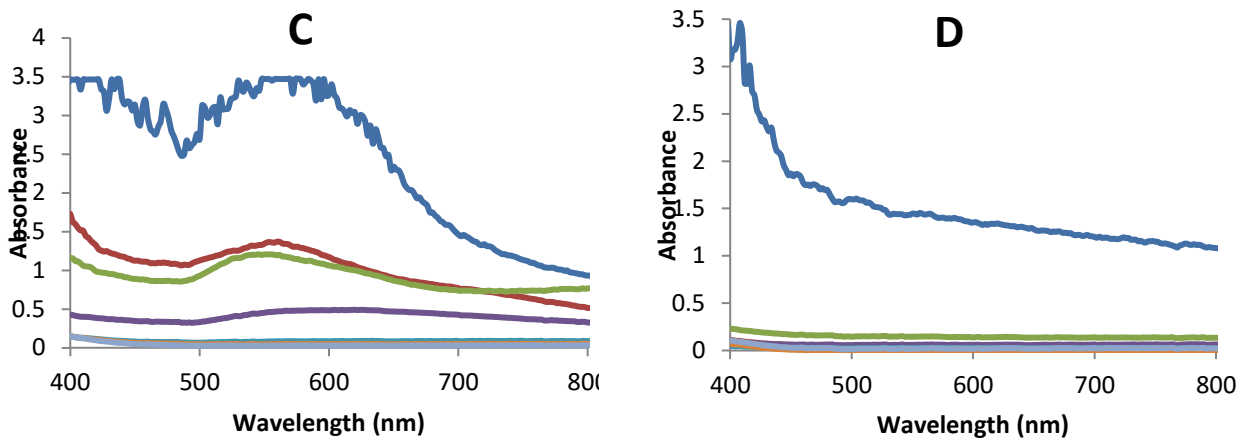


Figure 3.2.2: A UV-VIS spectra of the biosynthesized gold nanoparticles using different plant extract concentrations at different temperatures (a) at 25 °C, (b) at 50 °C, (c) 70 °C, and (d) at 100 °C.

### 3.2.3. The Effect of pH on the synthesis of *A.annua*-AuNPs

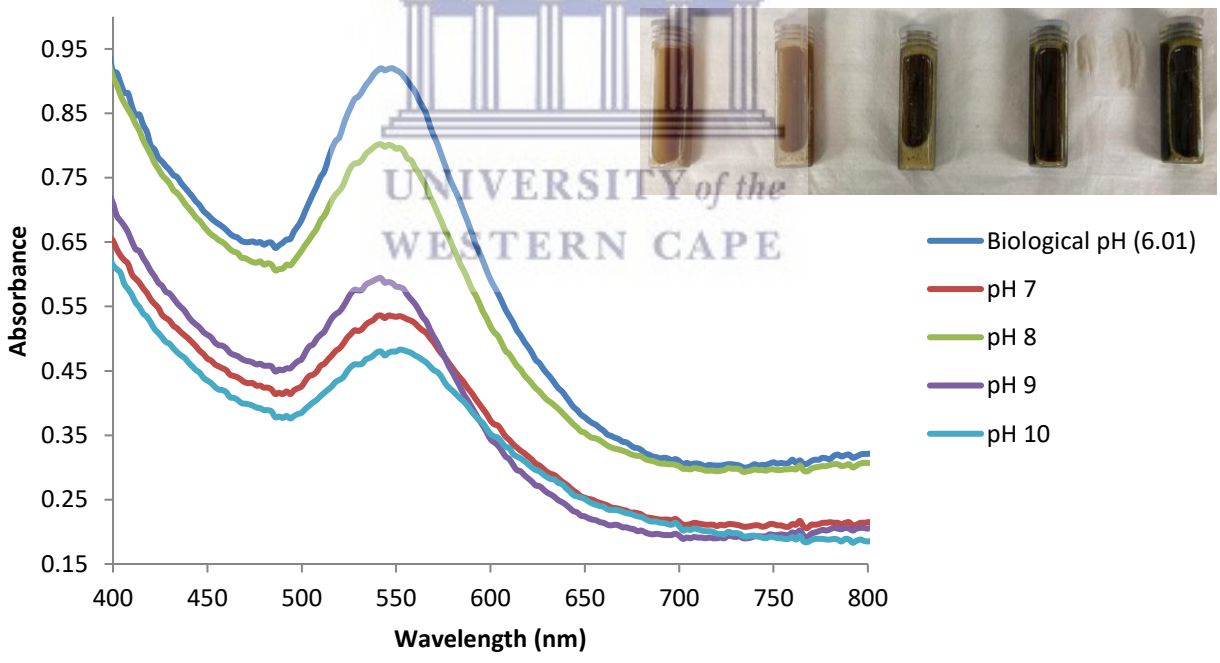


Figure 3.2.3: The UV-VIS spectra showing the effect of pH.

The biological pH of the *A.annua* plant extract was measured to be 6.01. The pH of the plant extracts was adjusted to 4 different pH levels (7-10) using 1 M sodium hydroxide (NaOH). NaOH has been previously reported to be used for adjusting the pH level of the AuNPs synthesized from the reduction of $HAuCl_4$ using *Hygrophila spinosa* aqueous extract (Satpathy et al., 2020). The UV absorbance spectra for synthesized AuNPs from *Artemisia annua* extract are shown in Figure 3.2.3. The wavelength for *Artemisia annua*-mediated AuNPs showed a maximum peak for the *A.annua*-AuNPs synthesized using biological pH (6.01). The pH level of 6 has been previously used and successfully produced green AuNPs with a diameter of 104 nm. This study also reviled that the synthesized AuNPs at pH level 6 had high colloidal stability shown by their Zeta potential of -28.96 mV (Ben Tahar et al., 2019). By increasing the pH the absorbance peak height decreases. This shows that an increase in pH results in a lower amount of *A.annua*-AuNPs. This observation is supported by the findings of Yang and colleagues. They synthesized AuNPs with controllable size using a green synthesis method. The 0.75 mM $HAuCl_4$ solution was reduced using fruit extracts from *Actini diadeliciosa*, *Malus domestica*, *Prunus persica*, and *Musa acuminate*. They adjusted their pH using NaOH from 3 to 6, 8, 10, and 11. The AuNPs synthesized from the *A. diadeliciosa* showed the maximum absorption peak at pH 6 and an increase in pH resulted in a decrease in their absorbance height intensity (Yang et al., 2017). To avoid the use of toxic solvents, the *Artemisia annua* aqueous plant extract was used without adjusting the pH level.



### 3.2.4. The Effect of Reaction time on the synthesis of *A.annua*-AuNPs.

The reaction time also affects the synthesis of AuNPs. By monitoring the height of maximum absorption ($\lambda_{max}$) we can deduce the starting time of the formation of A.annua-AuNPs as well as when the reaction starts to be constant or decrease. The *A.annua*-AuNPs started to form at 25 minutes of the incubation time. The incubation time of 1 hour produced AuNPs and to save energy it was used as an optimized incubation time.

### 3.3. Characterisation of the optimized *A.annua*-AuNPs

#### 3.3.1. UV-VIS analysis

AuNPs have unique optical properties that are sensitive to shape and size and also have a specific range of absorbance (Huong et al., 2021). Ultraviolet-Visible (UV-Vis) spectroscopy was used to check the surface plasmon resonance (SPR) spectra of the optimized AuNPs from the *A.annua* extract. As seen in Figure 3.3.1 (A), we were able to reduce gold (III) chloride precursor into gold nanoparticles using *Artemisia annua* plant extract. Shin and colleagues have synthesized the biogenic AuNPs using the hydrophilic silk sericin as a reducing and capping agent. They used UV-Vis to confirm the success in AuNP formation and found an absorbance around 525 nm which they accepted (Shin et al., 2022). The SPR peak (Figure 3.3.1 (A)) appeared to confirm the presence of AuNPs at a $\lambda_{max}$ ~550 nm which is in agreement with other previous studies that reported AuNPs SPR in a range between 500-600 nm (Basavegowda et al., 2014; Amale et al., 2021). The UV-VIS for *Artemisia annua* extracts was measured and is shown in Figure 3.3.1 (B). The results show the characteristic peaks at 300–400 nm and between 530–560 nm which corresponds to the artemisinin component. The UV-Vis analysis done by Ghaffoori and colleagues where they analyzed artemisinin from *A.annua* confirms these results (Gafoori et al. 2013). This observation shows the presence of an artemisinin compound in the prepared aqueous extract of *Artemisia annua* which is the most important phytochemical with medicinal properties such as antimicrobial, antibacterial, and anti-inflammatory properties (Mirbehbahani et al., 2020). The other peaks of the *Artemisia annua* extract at 476 and 502 nm may be assigned to other phytochemicals obtained in *A.annua* extract such as artemisinic acid, scopoletin, casticine, rosmarinic acid (Anshul et al. 2013). Furthermore, other overlapping peaks in a region of 480–510 nm may correspond to the green natural pigments in the *A.annua* plant. The report on the UV-VIS spectrum of *Artemisia annua* in Figure 3.3.1 (B) is in agreement with the study done by Mirbehbahani and colleagues when investigating *Artemisia annua* L extract (Mirbehbahani et al., 2020).

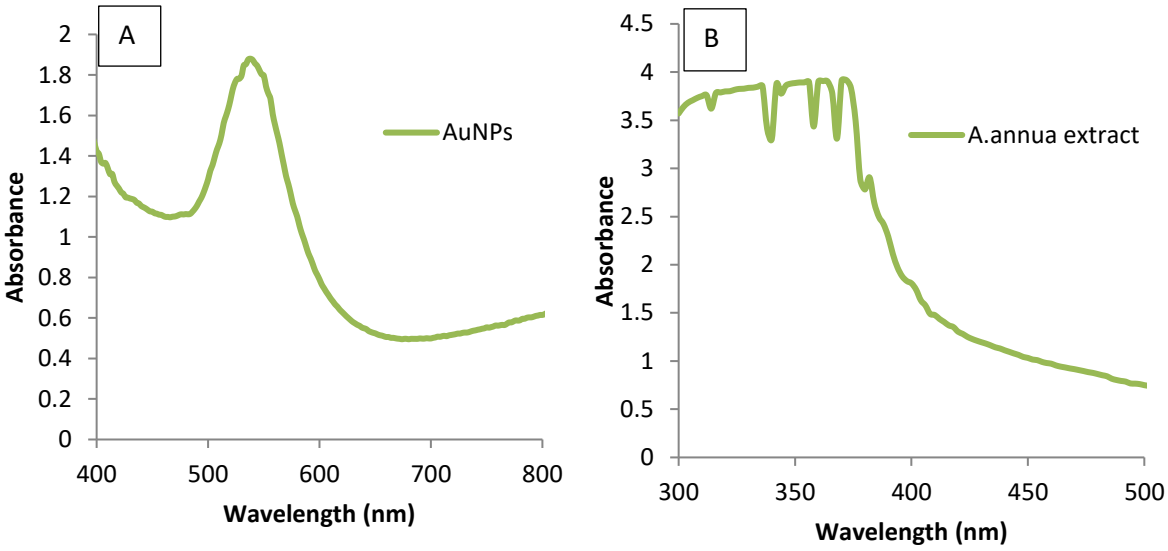


Figure 3.3.1: (A) UV-VIS spectrum of the optimized and washed AuNPs and (B) UV-VIS spectrum of Artemisia annua plant extract.

### 3.3.2. FTIR analysis

FTIR characterizations were carried out to identify possible functional groups in *A.annua* extract and AuNPs synthesized from *A.annua* and the results are shown in Figure 3.3.2. The spectra of *A.annua* extract and *A.annua*-AuNPs in Figure 3.3.2 revealed a strong band at 3436, 2080,2088, 1638, 676, and 622 $cm^{-1}$. These bands are characteristic bands that were also obtained by Basavegowda and colleagues where they synthesized gold and silver nanoparticles using *A.annua* plant extract. They obtained the FTIR spectra with strong absorption bands for *A.annua* and the synthesized AuNPs at 3366 and 3396, 2925 and 2925, 1643 and 1629, 1399 and 1383, and 1042 and 1070 $cm^{-1}$, respectively. Some of their bands had a shift which is also observed on our FTIR spectra and they deduce that it is caused by the protein binding (Basavegowda et al., 2014).

The band at 3436 $cm^{-1}$ in *A.annua* extract and AuNPs profiles was attributed to the hydroxyl group (~O-H) stretching for phenols or aromatic primary amine compounds. The small bands at 2080 and 2088 $cm^{-1}$ were attributed to the aromatic -C-H stretching. The sharp medium absorption peaks located at 1638 $cm^{-1}$ could be assigned to the carboxyl –C=O stretching. These functional groups are supported by Bogireddy and co-workers who synthesized gold nanoparticles using *Sterculia acuminata* extract and obtained a similar FTIR spectrum.

They also reported that the % Transmittance shows a decrease from before to after the reduction of their AuNPs at some of the peaks which indicates the phenolic compounds acted as a stabilizing agent via several functional groups (Bogireddy et al., 2015). This decrease in the %Transmittance is also observed in the synthesized *A.annua*-AuNPs. Furthermore, the 672 $cm^{-1}$ peaks are attributed to alkene (C=C) stretching. The peaks assigned to *Artemisia annua* are in agreement with studies done by Mirbehbahani and colleagues where they investigated the potential of *Artemisia annua* L. for wound healing effect (Mirbehbahani et al., 2020).

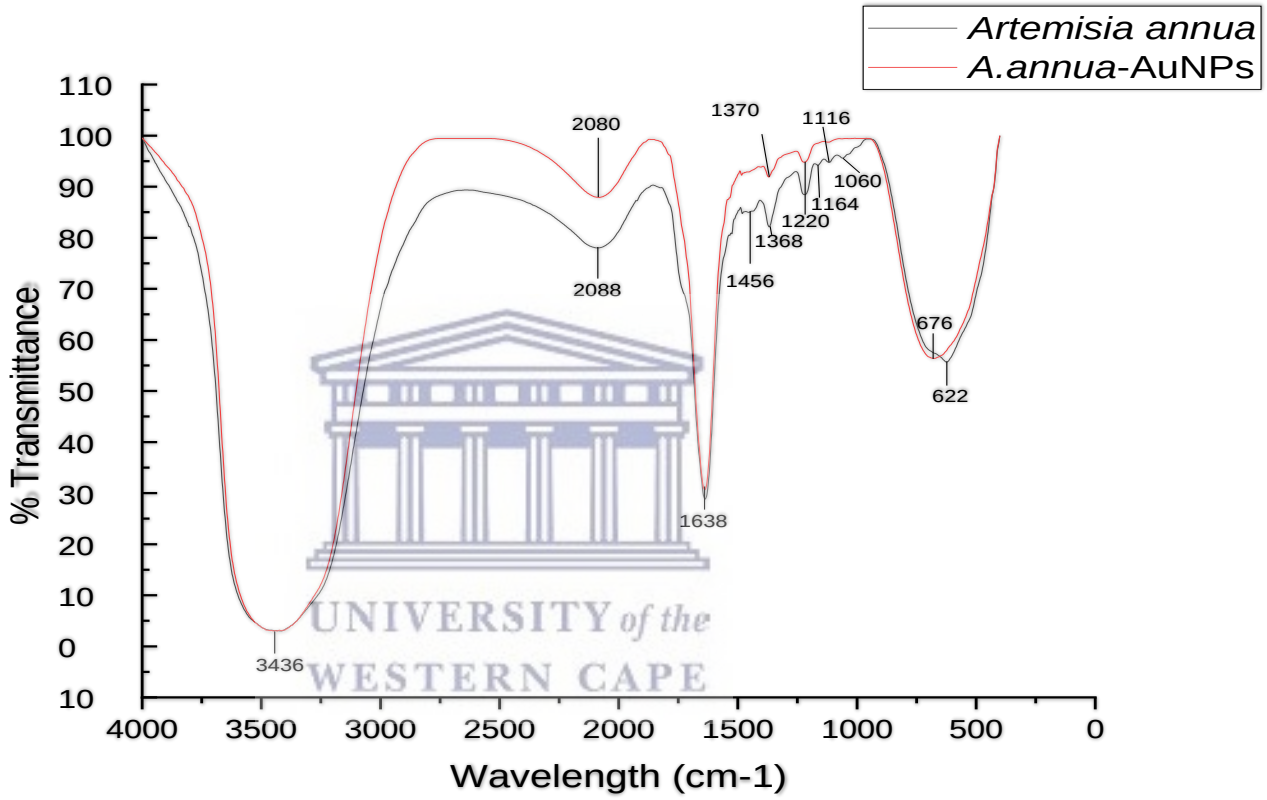


Figure 3.3.2: FTIR spectra showing the Artemisia annua (black) plant extract and A.annua-AuNPs (red)

### 3.3.3. DLS analysis

Dynamic light scattering technique was used to measure the size distribution, PDI, and zeta potential value of the phytochemically synthesized *A.annua*-AuNPs. The synthesis of *Artemisia*-mediated gold nanoparticles with optimized conditions as discussed in section 3.2 has produced AuNPs with different sizes and shapes. This is in agreement with previous studies, which also showed that the green synthesis of AuNPs at lower temperatures such as 25 ºC yielded larger AuNPs of different shapes and sizes (Elbagory et al., 2016). This fact is supported by Fanoro and co-workers who used *Combretum erythrophyllum* leaf extract to synthesize AuNPs at room temperature. They obtained *Combretum erythrophyllum* synthesized AuNPs of different sizes and shapes (Fanoro et al., 2021). The polydispersity index (PDI) represents the ratio of particles of different sizes to the total number of particles. A sample with a low PDI value (<0.1) is considered to be more monodispersed. Kumar and colleagues supported this fact. They synthesized AuNPs using a green synthesis approach where the oil from *Plukenetia volubilis* was used as a reducing agent. They considered a PDI value of 0.0665 for their AuNPs to be monodispersed (Kumar et al., 2016). Our synthesized *A.annua*-AuNPs had a PDI value of 0.479 ± 0.0174 showing that they are highly polydispersed when synthesized at 25 ºC due to the presence of quasi-spherical and irregular big AuNPs. This PDI value is supported by Dube and co-workers' where synthesized AuNPs using Salvia Africana-lutea and Sutherlandia frutescens and obtained a PDI value of 0.51 ± 0.03 (Dube et al., 2020). The stability of *A.annua*-AuNPs depends on both size and surface charge (zeta potential value) present on the AuNPs (Bergen et al., 2006). The zeta potential of -38.2 ± 1.77 shows the good stability and dispersity of our *A.annua*-AuNPs. This is in agreement with the study by Adoni and colleagues (Adoni et al., 2020) where they reported that a high negative value of AgNPs supports their good colloidal nature, high dispersity, and long-term stability due to negative-negative repulsion. Figure 3.3.2 shows the distribution by the intensity of *A.annua*-AuNPs. The majority of nanoparticles show an average of 107.94 ± 5.73 nm hydrodynamic radius.

Table 3: The Hydrodynamic radius, Polydispersity index (PDI), and Zeta potential value obtained from optimized *A.annua*-AuNPs.

| Sample name | Hydrodynamic radius (nm) | PDI | Zeta potential (mV) |
|---|---|---|---|
| *A. Annua*-AuNPs | 107.94 ±5.73 | 0.479±0.0174 | -38.2±1.77 |

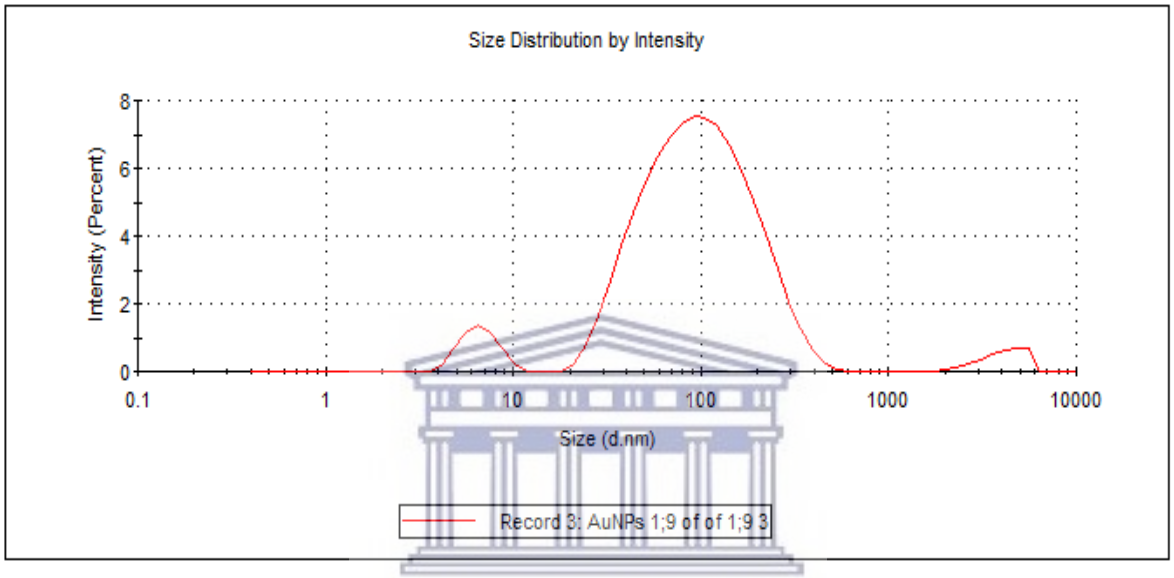


Figure 3.3.3: Particle size distribution for AuNPs produced from *A.annua*.



### 3.3.4. HRTEM analysis

A high-resolution transmission electron microscope was used to analyze the morphology and size of the gold nanoparticles produced using *A.annua*. A portion of *A.annua*-AuNPs solution was placed on a carbon-coated copper grid and allowed to dry under ambient conditions. HRTEM images were recorded at different magnifications (Figure 3.3.4 (A) 100 nm and (B) 20 nm). The HRTEM images of the AuNPs, produced from *Artemisia annua* plant extracts, show variable geometrical shapes and sizes. These various geometric shapes were also observed by Hosny and colleagues. They used both *A. halimus* and *C. amperosidies* extracts to phytosynthesize AuNPs at a temperature of 60 °C. Their HRTEM image showed a mixture of small spheres, triangles, and irregular polygons with average particles size ranging from 2-10 nm for *A. halimus*-AuNPs and up to 40 nm for *C. amperosidies*-AuNPs (Hosny et al., 2021). Figure 3.3.4 (A) shows that most of the *A.annua*-AuNPs have a spherical shape dominated and

a few triangular and irregularly shaped particles. Most of the irregular shapes and triangular AuNPs are bigger than spherical particles. Gold nanoparticles had sizes ranging from 10 to 60 nm, and most were ~50 nm as shown in the size distribution curve (Figure 3.3.4.D). The results of mixed shapes and sizes are in agreement with the size distribution by intensity (Figure 3.3.3). Overall, larger particles were mostly triangular and truncated triangular shaped. The formation of larger triangles and truncated triangle AuNPs was also obtained by Choudhary and co-workers who synthesized AuNPs using *Lagerstroemia speciosa* leaf extract for 30 minutes at 25 °C (Choudhary et al., 2017). On the other hand, the shape of AuNPs was also reported to be controlled by varying the concentrations of the reducing, growth-controlling, and stabilizing agents such as Gallatin. Suarasan and co-workers synthesized AuNPs in the presence of gelatin biopolymer. They obtained an HRTEM image with only triangular and some truncated triangular-shaped AuNPs when using a low gelatin concentration of 0.5% and only spherical AuNPs when using a high gelatin concentration (of 1.5 %) (Suarasan., 2015). Their synthesis differs from our *A.annua*-AuNPs synthesis by the use of gelatin biopolymer to reduce $HAuCl_4$ whereas our synthesis only involves the use of *A.annua* extract. Moreover, their incubation temperature was 80 °C for 6 hours and they produced AuNPs with an average diameter of 18 ± 3.5 nm which could have better potential to diffuse cells than our *A.annua*-AuNPs (50 nm) that were incubated for an hour at 25 °C. On the other hand, smaller nanoparticles were mostly, spherical, although a few small triangles could also be observed. As can be seen from the micrograph, there are also very long rod-shaped AuNPs. This mixture of geometrical shapes is very common for the green synthesis of AuNPs as reported before. It was also reported that plant extract contains a variety of phytochemicals which result in a variety of shapes (Mariychuk et al., 2020; Muthukumar et al., 2016).

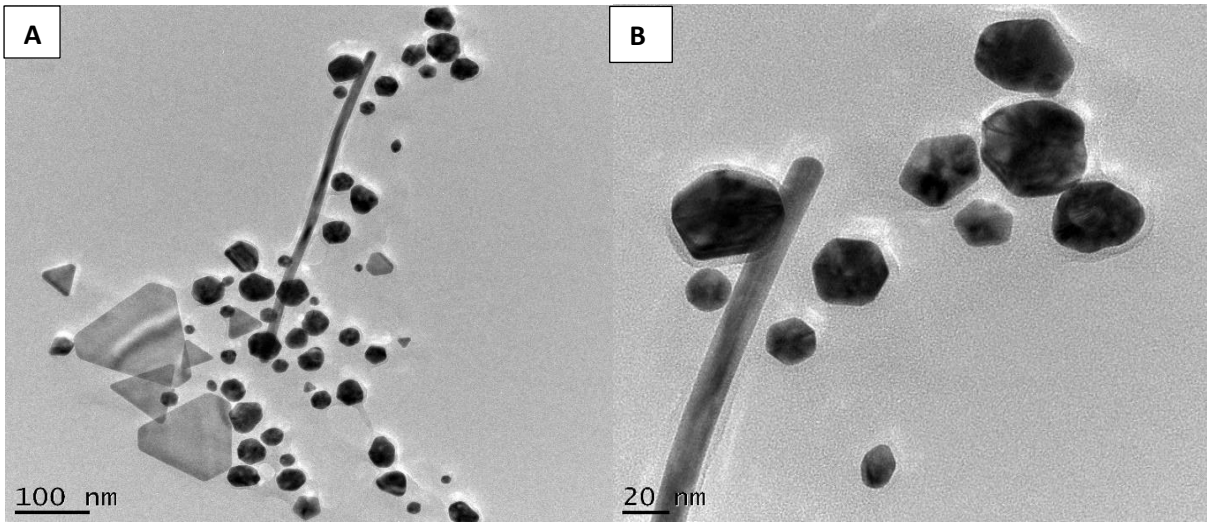

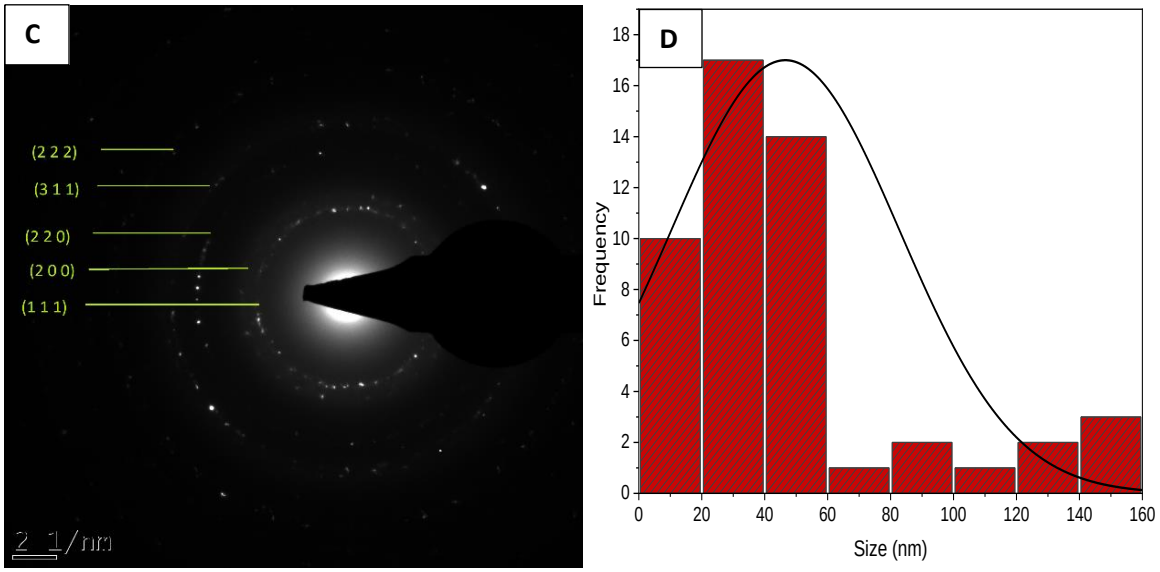


Figure 3.3.4: The TEM image at different magnifications (A) 100nm and (B) 20nm, (C) the crystalline patterns, and (D) the size distribution curve for the synthesized A.annua-AuNPS.

Table 4: Various numerical values obtained using Image J software to calculate d-spacing (Å) which was further used to obtain miller indices by comparing them with JCPDS card.

| Ring no. | 1/2r (1/nm) | 1/r (1/nm) | r (nm) | d-spacing (Å) | (hkl) |
|---|---|---|---|---|---|
| 1 | 8.474 | 4.237 | 0.236016 | 2.360160491 | (1 1 1) |
| 2 | 9.834 | 4.917 | 0.203376 | 2.033760423 | (2 0 0) |
| 3 | 13.826 | 6.913 | 0.144655 | 1.446549978 | (2 2 0) |
| 4 | 16.437 | 8.2185 | 0.121677 | 1.21676705 | (3 1 1) |
| 5 | 21.181 | 10.5905 | 0.094424 | 0.944242481 | (2 2 2) |

Figure 3.3.4 C shows the selected electron diffraction (SAED) pattern obtained from TEM images. The Image J software was used together with Joint Committee on Powder Diffraction Standards (JCPDS no. 04-0784) card to get the miller indices. *A.annua*-AuNPs revealed circular rings relating to the (111), (200), (220), (311), and (222) planes which confirmed *A.annua*-AuNPs crystalline properties. Gopalakrishnan and Raghu have synthesized AuNPs synthesized using *Silybum marianum* seed extract and investigated their crystalline nature using SAED. Their results concluded that the crystalline nature of AuNPs is shown by the

circular patterns that correspond to reflections from (1 1 1), (2 0 0), (2 2 0), and (3 1 1) sets of lattice planes (Gopalakrishnan and Raghu., 2014).

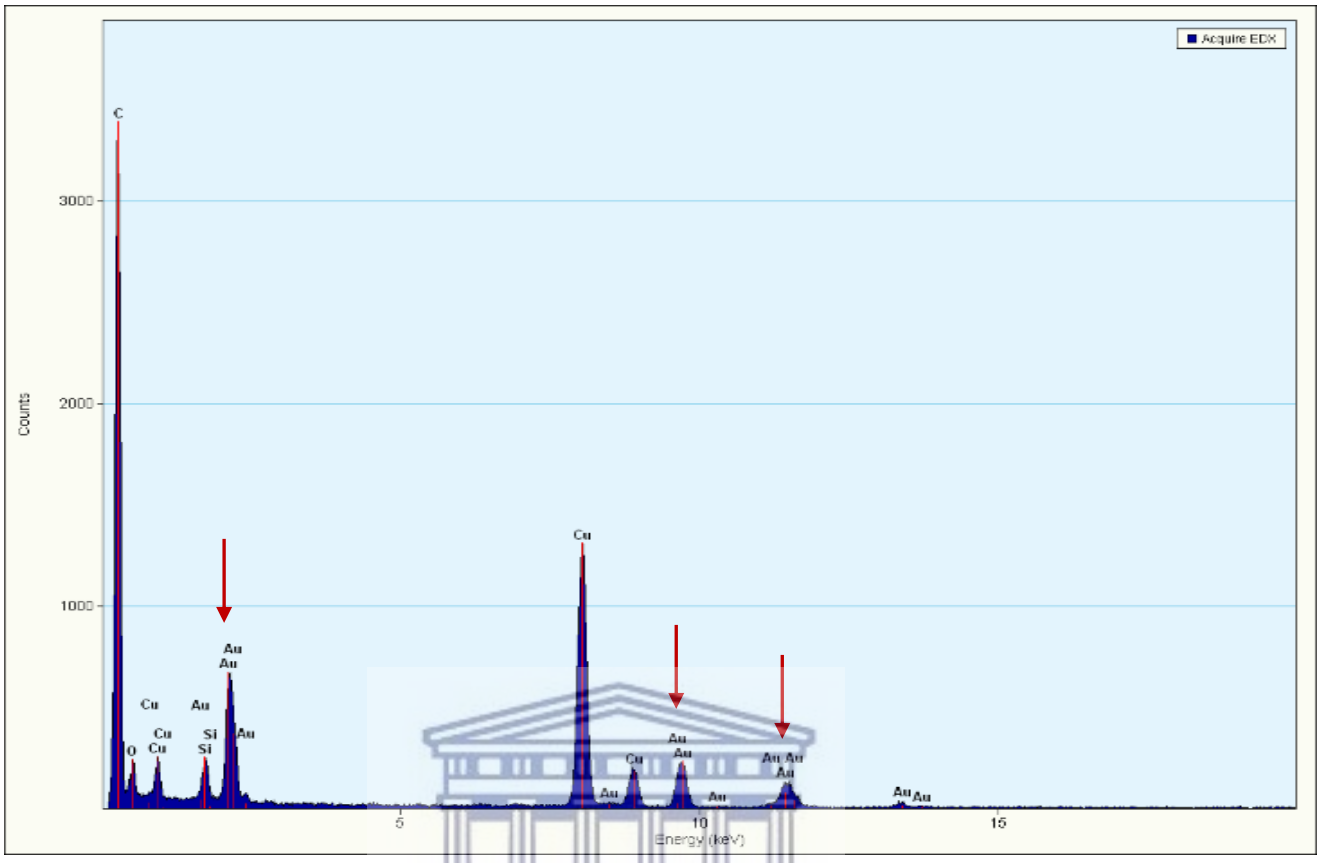


Figure 3.3.5. The EDX spectroscopy analysis of A.annua-AuNPs.

The EDX spectroscopy analysis of the AuNPs confirmed the presence of gold ions in the samples selected for HRTEM analysis. Strong optical adsorption peaks were observed at around 2.5, 9.7, and 11.4 KeV (Figure 3.2.4.3), which is consistent with a previous study by Vo and colleagues. They synthesized AuNPs using leaf extract of *A. assamica* . They obtained an EDX spectrum with the highest Au signal at 2.13, 8.45, and 9.73 KeV. It was also concluded that the peaks corresponding to carbon and oxygen may come from the phytochemicals capping on the gold nanoparticles (Vo et al., 2020). These findings were also supported by Basavegowda and co-workers where their EDX spectra showed strong absorption of Au at ~2.22 keV which was said to be due to the surface plasmon resonance of AuNPs. They further supported the fact that the presence of strong peaks of carbon, copper, and silicon in the EDX spectrum is attributed to the HRTEM carbon-coated copper grid used for the analysis and the detector window. Moreover, the presence of oxygen was suggested to be due to traces of the phytochemicals of the *A.annua* extracts and the gold salt (Basavegowda et al., 2014).

### 3.4. Stability of *A.annua*-AuNPs in LB broth and MHB

For any biological application, nanoparticles are required to be stable in any biological environment. When nanoparticles with poor stability are introduced into a biological media, there is a possibility of aggregation which alters their properties hence affecting the biological activity. Therefore, it was important to confirm the stability of *A.annua*-AuNPs in biological environments. The stability of *A.annua*-AuNPs was evaluated on LB broth and MHB over 24 hours. Moreover, the stability of the *A.annua*-AuNPs was evaluated at 25 and 37 ºC to further investigate their effect on stability. This choice of biological media and incubation temperatures was due to their wide use in biological assays such as bacteria culture. Tyavambiza and colleagues evaluated the stability of green AgNPs using 25 and 37 ºC for 24 h and used the UV-Vis to evaluate (Tyavambiza et al., 2016). The UV-Vis for the synthesized *A.annua*-AuNPs to evaluate the stability is reported in Figure 3.3.6.

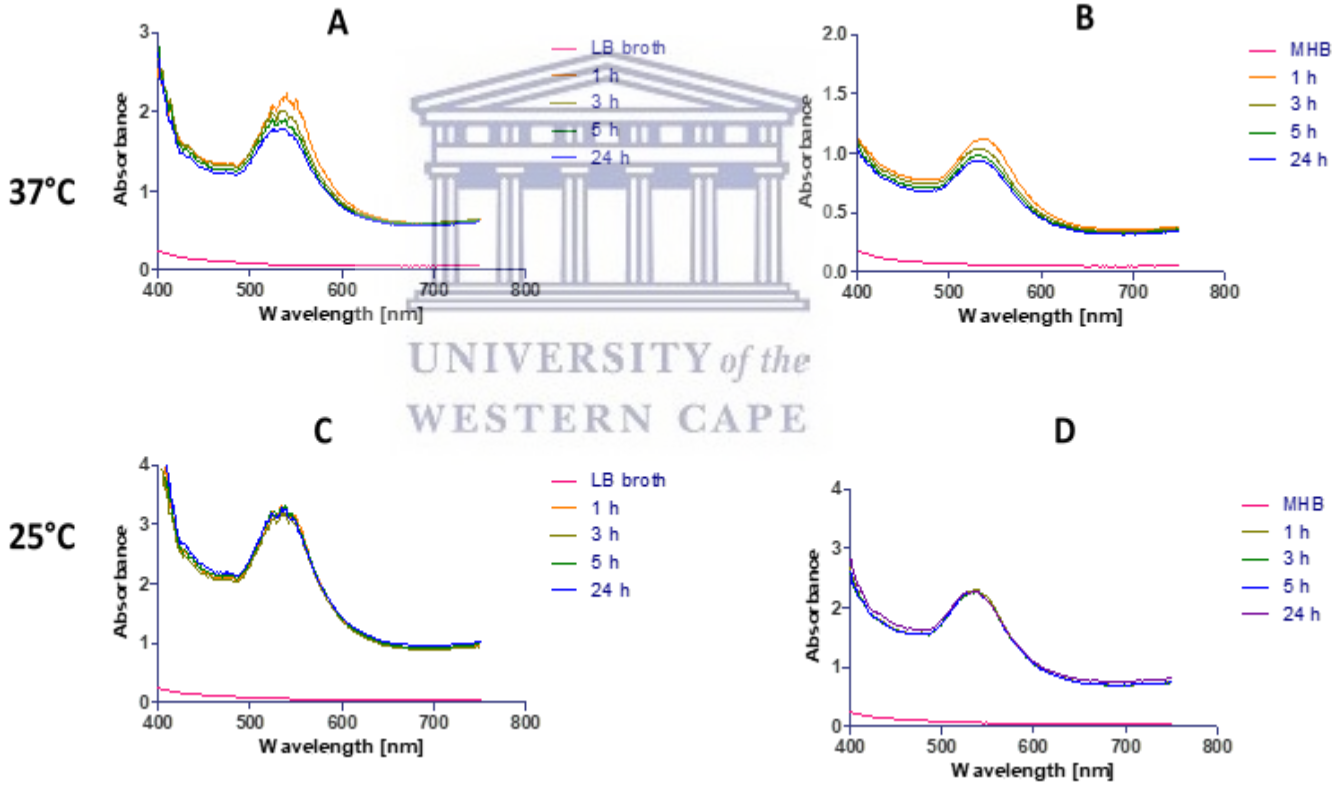


Figure 3.3.6: The UV-Vis spectra of *A.annua*-AuNPs, recorded over a 24 h period (at 25 and 37 ºC) after mixing with different biological media; (A, C) LB broth and (B, D) MHB.

The UV-VIS absorption spectra show that the SPR of the *A.annua*-AuNPs at 37 ºC shows a significant decrease in absorbance as the time of incubation is increased for both LB-broth and MHB, implying that they are not stable at 37 ºC. On the other hand, the *A.annua*-AuNPs were stable at 25ºC for both biological media which is shown by the overlapping UV-VIS absorption peaks (Figure 3.3.6 C and D). The incubation temperature of 25 ºC and MHB were used for antimicrobial application.

### 3.5. The Antimicrobial Activity of *A.annua*-AuNPs

The antimicrobial activity of *A.annua*-AuNPs was investigated against a total of six pathogenic microbes namely *S. aureus*, *S. epidermidis*, MRSA, *K. pneumoniae*, *E. coli*, and *P. aeruginosa* using agar well diffusion method. The activity was conducted by evaluating MIC and the zones of inhibition in mm around each disc containing the synthesized AuNPs, *Artemisia annua* water extract, and Ciprofloxacin as a positive control (Figure 3.3.7). The presence of the inhibition zone shows a positive activity and the results are shown in Tables 5 & 6.

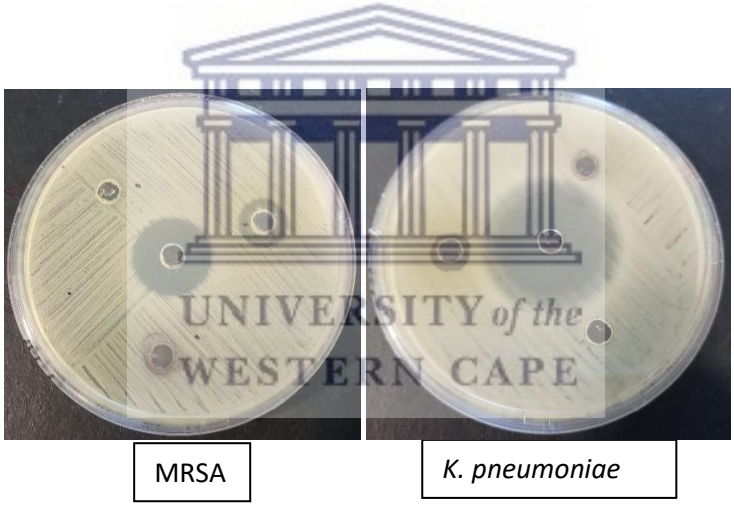


Figure 3.3.7: Antimicrobial activity of biosynthesized *A.annua*-AuNPs from *A. annua* extract with activity on Gram positive (MRSA) and Gram-negative (*K.pneumoniae*).

Table 5. The results of antimicrobial activity with zones of inhibition

| Microorganisms | Zones of inhibition (mm) | | |
|---|---|---|---|
| | Water extract | AuNPs | Ciprofloxacin |
| *S. aureus* | - | - | 22 |
| *S. epidermidis* | 15 | - | 27 |
| MRSA | 13 | - | 21 |
| *K. pnuemoniae* | 10 | - | 28 |
| *E. coli* | - | - | 34 |
| *P. aeruginosa* | - | - | 24 |

Table 6: The antimicrobial results using the minimum inhibitory assay (MIC).

| | MIC (µg/ml) | | |
|---|---|---|---|
| Microorganisms | Water extract | AuNPs | Ciprofloxacin |
| *S. aureus* | <1000 | 275 | 0.5 |
| *S. epidermidis* | <1000 | 275 | 0.25 |
| MRSA | <1000 | 550 | 0.5 |
| *K. pnuemoniae* | <1000 | 137 | 0.02 |
| *E. coli* | <1000 | 137 | 0.02 |
| *P. aeruginosa* | <1000 | - | 0.5 |



This study found that water extracts of *Artemisia annua* displayed significant antibacterial activity against *S. epidermidis*, MRSA, and *K. pnuemoniae* by showing inhibition zone of 15, 13, and 10 mm respectively. There was no zone of inhibition observed for *S. aureus, E. coli*, and *P. aeruginosa* microorganisms. These results are in agreement with a previous study, which reported that water extracts of *A.annua* showed low antibacterial properties but better antifungal properties against *C.albicans* (Johnson et al., 2014). Mirbehbahani and colleagues have reported the tendency of *A.annua* water extract to have an unclear zone of inhibition which is caused by the diffusion of green-color pigments into an agar medium (Mirbehbahani et al., 2020). This phenomenon could result in *A.annua* being reported inactive for some

microorganisms. Furthermore, artemisinin contained in *A.annua* extract has been reported as the main component that results in the antimicrobial property of the species of interest (Kim et al., 2015). The low amount or concentration of this component could result in poor antimicrobial activity of the *A.annua* water extract.

The zone of inhibition of the synthesized *A.annua*-AuNPs against all tested microorganisms was not visible. The *A.annua*-AuNPs were mostly active on *K. pnuemoniae* and *E.coli*, both with MIC values of 137 µg/ml. Another same inhibition activity of *A.annua*-AuNPs was observed against *S. epidermidis* and *S. aureus*, with a MIC value of 275 µg/ml. The lowest activity recorded for *A.annua*-AuNPs was against MRSA, with a MIC value of 550 µg/ml. The antimicrobial activity of *A.annua*-AuNPs compared to that of the positive control (Ciprofloxacin) shows that the biosynthesized AuNPs have low antimicrobial activity. Very low concentrations of Ciprofloxacin are required to inhibit the tested microorganisms hence showing that the *A.annua*-AuNPs did not have good antimicrobial properties.

The determinants of antimicrobial activity of AuNPs are determined by size, concentration, purification, and surface modifications. There was no purification method used on the synthesized AuNPs which could have caused a negative impact on antimicrobial activity. These results support the report that the antibacterial activity of AuNPs is not part of their characteristics. AuNPs are also considered to be biologically inert (Allahverdiyev et al., 2011). Furthermore, Zhang and associates have supported this fact based on AuNPs generally having higher MIC values and very small inhibition zones when compared to Silver nanoparticles (AgNPs) (Zhang et al., 2015). Hernández-Sierra and colleagues did a comparison of antibacterial activity on both AuNPs (80 nm) and AgNPs (25 nm) against *S. aureus*. AgNPs had a MIC of 4.86 ± 2.71 µg/mL whereas AuNPs started to show an inhibition at a very high concentration (197 µg/mL) (Hernández-Sierra et al., 2008).

**References**

Acharya, P., Jayaprakasha, G.K., Crosby, K.M., Jifon, J.L. and Patil, B.S., 2019. Green-synthesized nanoparticles enhanced seedling growth, yield, and quality of onion (Allium cepa L.). ACS Sustainable Chemistry & Engineering, 7(17), pp.14580-14590.

Adoni, M., Yadam, M., Gaddam, S.A., Rayalacheruvu, U. and Kotakadi, V.S., 2020. Antimicrobial, antioxidant, and dye degradation properties of biosynthesized silver nanoparticles from Artemisia annua L. Lett. Appl. NanoBioScience, 10, pp.1981-1992.

Akintelu, S.A., Yao, B. and Folorunso, A.S., 2021. Green synthesis, characterization, and antibacterial investigation of synthesized gold nanoparticles (AuNPs) from Garcinia kola pulp extract. Plasmonics, 16(1), pp.157-165.

Allahverdiyev, A.M., Kon, K.V., Abamor, E.S., Bagirova, M. and Rafailovich, M., 2011. Coping with antibiotic resistance: combining nanoparticles with antibiotics and other antimicrobial agents. Expert review of anti-infective therapy, 9(11), pp.1035-1052.

Amale, F.R., Ferdowsian, S., Hajrasouliha, S., Kazempoor, R., Mirzaie, A., Dakkali, M.S., Akbarzadeh, I., Meybodi, S.M. and Mirghafouri, M., 2021. Gold nanoparticles loaded into niosomes: A novel approach for enhanced antitumor activity against human ovarian cancer. Advanced Powder Technology, 32(12), pp.4711-4722.

Anshul N, Bhakuni RS, Gaur R, Singh D (2013) Isomeric flavonoids of Artemisia annua(Asterales: Asteraceae) as insect growth inhibitors against Helicoverpa armigera (Lepidoptera: Noctuidae) Florida. Entomologist 96:897–903

Asnag, G.M., Oraby, A.H. and Abdelghany, A.M., 2019. Green synthesis of gold nanoparticles and its effect on the optical, thermal and electrical properties of carboxymethyl cellulose. Composites Part B: Engineering, 172, pp.436-446.

Basavegowda, N., Idhayadhulla, A. and Lee, Y.R., 2014. Preparation of Au and Ag nanoparticles using Artemisia annua and their in vitro antibacterial and tyrosinase inhibitory activities. Materials Science and Engineering: C, 43, pp.58-64.

Ben Tahar, I., Fickers, P., Dziedzic, A., Płoch, D., Skóra, B. and Kus-Liśkiewicz, M., 2019. Green pyomelanin-mediated synthesis of gold nanoparticles: Modelling and design, physico-chemical and biological characteristics. *Microbial cell factories*, *18*(1), pp.1-11.

Bergen, J.M., Von Recum, H.A., Goodman, T.T., Massey, A.P. and Pun, S.H., 2006. Gold nanoparticles as a versatile platform for optimizing physicochemical parameters for targeted drug delivery. Macromolecular bioscience, 6(7), pp.506-516.

Bindhu, M.R. and Umadevi, M., 2014. Antibacterial activities of green synthesized gold nanoparticles. *Materials Letters*, *120*, pp.122-125.

Bogireddy, N.K.R., Anand, K.K.H. and Mandal, B.K., 2015. Gold nanoparticles—synthesis by Sterculia acuminata extract and its catalytic efficiency in alleviating different organic dyes. *Journal of Molecular Liquids*, *211*, pp.868-875.

Burton, D., 2013. Collision Theory in Developmental Relationship. *Journal of Unification Studies Vol*, *14*, pp.145-162.

Choudhary, B.C., Paul, D., Gupta, T., Tetgure, S.R., Garole, V.J., Borse, A.U. and Garole, D.J., 2017. Photocatalytic reduction of organic pollutant under visible light by green route synthesized gold nanoparticles. *Journal of Environmental Sciences*, *55*, pp.236-246.

Das, R.K., Gogoi, N. and Bora, U., 2011. Green synthesis of gold nanoparticles using Nyctanthes arbortristis flower extract. *Bioprocess and biosystems engineering*, *34*(5), pp.615-619.

De Souza, C.D., Nogueira, B.R. and Rostelato, M.E.C., 2019. Review of the methodologies used in the synthesis gold nanoparticles by chemical reduction. *Journal of Alloys and Compounds*, *798*, pp.714-740.

Deepak, V., Umamaheshwaran, P.S., Guhan, K., Nanthini, R.A., Krithiga, B., Jaithoon, N.M.H. and Gurunathan, S., 2011. Synthesis of gold and silver nanoparticles using purified URAK. *Colloids and Surfaces B: Biointerfaces*, *86*(2), pp.353-358.

Dube, P., Meyer, S., Madiehe, A. and Meyer, M., 2020. Antibacterial activity of biogenic silver and gold nanoparticles synthesized from Salvia africana-lutea and Sutherlandia frutescens. Nanotechnology, 31(50), p.505607.

Dubey, S.P., Lahtinen, M. and Sillanpää, M., 2010. Green synthesis and characterizations of silver and gold nanoparticles using leaf extract of Rosa rugosa. *Colloids and Surfaces A: Physicochemical and Engineering Aspects*, *364*(1-3), pp.34-41.

Elbagory, A.M., Cupido, C.N., Meyer, M. and Hussein, A.A., 2016. Large scale screening of southern African plant extracts for the green synthesis of gold nanoparticles using microtitre-plate method. Molecules, 21(11), p.1498.

ElMitwalli, O.S., Barakat, O.A., Daoud, R.M., Akhtar, S. and Henari, F.Z., 2020. Green synthesis of gold nanoparticles using cinnamon bark extract, characterization, and fluorescence activity in Au/eosin Y assemblies. Journal of Nanoparticle Research, 22(10), pp.1-9.

Fadaka, A., Aluko, O., Awawu, S. and Theledi, K., 2021. Green synthesis of gold nanoparticles using Pimenta dioica leaves aqueous extract and their application as photocatalyst, antioxidant, and antibacterial agents. Journal of Multidisciplinary Applied Natural Science, 1(2).

Fanoro, O.T., Parani, S., Maluleke, R., Lebepe, T.C., Varghese, J.R., Mavumengwana, V. and Oluwafemi, O.S., 2021. Facile Green, Room-Temperature Synthesis of Gold Nanoparticles Using Combretum erythrophyllum Leaf Extract: Antibacterial and Cell Viability Studies against Normal and Cancerous Cells. Antibiotics, 10(8), p.893.

Fu, C., Yu, P., Wang, M. and Qiu, F., 2020. Phytochemical analysis and geographic assessment of flavonoids, coumarins and sesquiterpenes in Artemisia annua L. based on HPLC-DAD quantification and LC-ESI-QTOF-MS/MS confirmation. *Food Chemistry*, *312*, p.126070.

Fuller, M.A. and Köper, I., 2019. Biomedical applications of polyelectrolyte coated spherical gold nanoparticles. *Nano convergence*, *6*(1), pp.1-10.

Gafoori H, Sariri R, Naghavi MR, Aryakia E, Dolatyari A, Shahzadeh Fazli SA, Ramazani H, Farahmand (2013) Analysis of artemisinin isolated from Artemisia annua L. by TLC and HPLC. J Liq Chromat Relat Technol 36:1198–1206

Geethalakshmi, R. and Sarada, D.V.L., 2013. Characterization and antimicrobial activity of gold and silver nanoparticles synthesized using saponin isolated from Trianthema decandra L. *Industrial Crops and Products*, *51*, pp.107-115.

Gopalakrishnan, R. and Raghu, K., 2014. Biosynthesis and characterization of gold and silver nanoparticles using milk thistle (Silybum marianum) seed extract. Journal of Nanoscience, 2014.

Gürsoy, N., Öztürk, B.Y. and Dağ, İ., 2021. Synthesis of intracellular and extracellular gold nanoparticles with a green machine and its antifungal activity. Turkish Journal of Biology, 45(2), pp.196-213.

Hasan, S., 2015. A review on nanoparticles: their synthesis and types. *Res. J. Recent Sci*, *2277*, p.2502.

Hernández-Sierra, J.F., Ruiz, F., Pena, D.C.C., Martínez-Gutiérrez, F., Martínez, A.E., Guillén, A.D.J.P., Tapia-Pérez, H. and Castañón, G.M., 2008. The antimicrobial sensitivity of

Streptococcus mutans to nanoparticles of silver, zinc oxide, and gold. Nanomedicine: Nanotechnology, Biology and Medicine, 4(3), pp.237-240.

Hosny, M., Fawzy, M., Abdelfatah, A.M., Fawzy, E.E. and Eltaweil, A.S., 2021. Comparative study on the potentialities of two halophytic species in the green synthesis of gold nanoparticles and their anticancer, antioxidant and catalytic efficiencies. *Advanced Powder Technology*, *32*(9), pp.3220-3233.

Huang, X., Wu, H., Liao, X. and Shi, B., 2010. One-step, size-controlled synthesis of gold nanoparticles at room temperature using plant tannin. *Green Chemistry*, *12*(3), pp.395-399.

Huong, V.T., Ta, H.K.T., Mai, N.X.D., Van Tran, T.T., Khuyen, B.X., Lee, N.Y., Phan, B.T. and Tran, N.H.T., 2021. Development of a highly sensitive sensor chip using optical diagnostic based on functionalized plasmonically active AuNPs. Nanotechnology, 32(33), p.335505.

Islam, N.U., Jalil, K., Shahid, M., Muhammad, N. and Rauf, A., 2019. Pistacia integerrima gall extract mediated green synthesis of gold nanoparticles and their biological activities. *Arabian Journal of Chemistry*, *12*(8), pp.2310-2319.

Johnson, A.S., Obot, I.B. and Ukpong, U.S., 2014. Green synthesis of silver nanoparticles using Artemisia annua and Sida acuta leaves extract and their antimicrobial, antioxidant and corrosion inhibition potentials. J. Mater. Environ. Sci, 5(3), pp.899-906.

Kim, W.S., Choi, W.J., Lee, S., Kim, W.J., Lee, D.C., Sohn, U.D., Shin, H.S. and Kim, W., 2015. Anti-inflammatory, antioxidant and antimicrobial effects of artemisinin extracts from Artemisia annua L. The Korean journal of physiology & pharmacology: official journal of the Korean Physiological Society and the Korean Society of Pharmacology, 19(1), p.21.

Kumar, B., Smita, K., Cumbal, L. and Debut, A., 2016. One pot synthesis and characterization of gold nanocatalyst using Sacha inchi (Plukenetia volubilis) oil: Green approach. *Journal of Photochemistry and Photobiology B: Biology*, *158*, pp.55-60.

Madhusudhan, A., Reddy, G.B. and Krishana, I.M., 2019. Green synthesis of gold nanoparticles by using natural gums. In Nanomaterials and plant potential (pp. 111-134). Springer, Cham.

Mariychuk, R., Grulova, D., Grishchenko, L.M., Linnik, R.P. and Lisnyak, V.V., 2020. Green synthesis of non-spherical gold nanoparticles using Solidago canadensis L. extract. Applied Nanoscience, 10(12), pp.4817-4826.

Mirbehbahani, F.S., Hejazi, F., Najmoddin, N. and Asefnejad, A., 2020. Artemisia annua L. as a promising medicinal plant for powerful wound healing applications. Progress in Biomaterials, 9(3), pp.139-151.

Mirbehbahani, F.S., Hejazi, F., Najmoddin, N. and Asefnejad, A., 2020. Artemisia annua L. as a promising medicinal plant for powerful wound healing applications. Progress in Biomaterials, 9(3), pp.139-151.

Muthukumar, T., Sambandam, B., Aravinthan, A., Sastry, T.P. and Kim, J.H., 2016. Green synthesis of gold nanoparticles and their enhanced synergistic antitumor activity using HepG2 and MCF7 cells and its antibacterial effects. Process Biochemistry, 51(3), pp.384-391.

Nayak, S., Sajankila, S.P. and Rao, C.V., 2021. Green synthesis of gold nanoparticles from banana pith extract and its evaluation of antibacterial activity and catalytic reduction of malachite green dye. Journal of Microbiology, Biotechnology and Food Sciences, 2021, pp.641-645.

Olga, M., Jana, M., Anna, M., Irena, K., Jan, M. and Alena, Č., 2022. Antimicrobial properties and applications of metal nanoparticles biosynthesized by green methods. *Biotechnology Advances*, p.107905.

Prema, P., Boobalan, T., Arun, A., Rameshkumar, K., Babu, R.S., Veeramanikandan, V., Nguyen, V.H. and Balaji, P., 2022. Green tea extract mediated biogenic synthesis of gold nanoparticles with potent anti-proliferative effect against PC-3 human prostate cancer cells. *Materials Letters*, *306*, p.130882.



Safari, K., Yadegari, M. and Hamedi, B., 2019. Effects of climate and soil properties on phytochemical characteristics of Ferulago angulate (Schltdl.) Boiss. Iranian Journal of Plant Physiology, 9(2), pp.2719-2726.

Satpathy, S., Patra, A., Ahirwar, B. and Hussain, M.D., 2020. Process optimization for green synthesis of gold nanoparticles mediated by extract of Hygrophila spinosa T. Anders and their biological applications. *Physica E: Low-dimensional Systems and Nanostructures*, *121*, p.113830.

Shajari, D., Bahari, A., Gill, P. and Mohseni, M., 2017. Synthesis and tuning of gold nanorods with surface plasmon resonance. Optical Materials, 64, pp.376-383.

Shin, M., Yang, S., Kwak, H.W. and Lee, K.H., 2022. Synthesis of gold nanoparticles using silk sericin as a green reducing and capping agent. *European Polymer Journal*, *164*, p.110960.

Suarasan, S., Focsan, M., Soritau, O., Maniu, D. and Astilean, S., 2015. One-pot, green synthesis of gold nanoparticles by gelatin and investigation of their biological effects on Osteoblast cells. *Colloids and Surfaces B: Biointerfaces*, *132*, pp.122-131.

Subara, D. and Jaswir, I., 2018. Gold nanoparticles: synthesis and application for Halal authentication in meat and meat products. *Int J Adv Sci Eng Inf Technol*, *8*, pp.1633-1641.

Suman, T.Y., Rajasree, S.R., Ramkumar, R., Rajthilak, C. and Perumal, P., 2014. The Green synthesis of gold nanoparticles using an aqueous root extract of Morinda citrifolia L. *Spectrochimica Acta Part A: Molecular and Biomolecular Spectroscopy*, *118*, pp.11-16.

Tyavambiza, C., Elbagory, A.M., Madiehe, A.M., Meyer, M. and Meyer, S., 2021. The antimicrobial and anti-inflammatory effects of silver nanoparticles synthesised from Cotyledon orbiculata aqueous extract. Nanomaterials, 11(5), p.1343.

Vo, T.T., Dang, C.H., Doan, V.D., Dang, V.S. and Nguyen, T.D., 2020. Biogenic synthesis of silver and gold nanoparticles from Lactuca indica leaf extract and their application in catalytic degradation of toxic compounds. Journal of Inorganic and Organometallic Polymers and Materials, 30(2), pp.388-399.

Yang, B., Chou, J., Dong, X., Qu, C., Yu, Q., Lee, K.J. and Harvey, N., 2017. Size-controlled green synthesis of highly stable and uniform small to ultrasmall gold nanoparticles by controlling reaction steps and pH. *The Journal of Physical Chemistry C*, *121*(16), pp.8961-8967.

Zhang, Y., Shareena Dasari, T.P., Deng, H. and Yu, H., 2015. Antimicrobial activity of gold nanoparticles and ionic gold. Journal of Environmental Science and Health, Part C, 33(3), pp.286-327.

# Chapter 4: Conclusion and recommendations

## 4.1. Conclusion

AuNPs were successfully synthesized using *A.annua* aqueous extract via a one-step biosynthesis method of the reduction of $HAuCl_4 \cdot XH_2O$. The synthesis was optimized by varying reaction parameters such as time, temperature, $HAuCl_4 \cdot XH_2O$, and plant extract concentrations. UV-VIS spectroscopy was used to monitor the effect that the mentioned parameters have on the synthesis of *A.annua*-AuNPs. The upscaled *A.annua*-AuNPs were fully characterized using UV-VIS, FTIR, DLS, and HRTEM to determine their physicochemical properties such as morphology and stability. The SPR peak for the formulated *A.annua*-AuNPs was observed at 550 nm which is within the specified range of the AuNPs. The FTIR spectra of A.annua-AuNPs showed characteristic peaks at 3436, 2088, 1638, and 676 $cm^{-1}$ which corresponds to the hydroxyl group (~O-H), C-H stretching, Cyanide (C=N) stretching, and alkene (C=C) stretching respectively. The DLS analysis showed that the *A.annua*-AuNPs were highly polydispersed with a PDI value of 0.479 ± 0.0174 and the negative zeta potential showing good stability. The HRTEM showed a variety of shapes and sizes with the quasi-spherical shape dominating with triangles and other irregular shapes having bigger sizes.

After the full characterization of *A.annua*-AuNPs, they were evaluated for stability in the biological media (LB-broth and MHB) at different temperatures. *A.annua*-AuNPs were found to be stable at 25 ℃ by showing no shift of the SPR peak. The evaluation of *A.annua*-AuNPs antimicrobial activity on 6 different bacterial strains showed the most activity on *K. pnuemoniae* and *E.coli,* both with MIC value of 137 µg/ml. The lowest activity was observed on MRSA, with a MIC value of 550 µg/ml. Comparing *A.annua*-AuNPs with the Ciprofloxacin (positive control) showed that high concentrations of A.annua-AuNPs are needed to inhibit the tested microorganisms. This has been reported to be related to the determinants of antimicrobial activity such as surface modification and purification methods. In conclusion, the aim to synthesize AuNPs using the bioreduction method with Artemisia annua as a reducing agent was a success. Furthermore, the antimicrobial activity will be enhanced and more details are provided in future work and recommendations. The major contribution of this research project was the investigation of the antibacterial property that *Artemisia annua* plant extract and *A.annua*-AuNPs possess making them potential drugs against antimicrobial resistance.

### 4.2. Recommendations

The modification of AuNPs with various molecules could make it an active antimicrobial agent. AuNPs have been reported to have a strong affinity for the sulfur atom (S) so coating the surface of *A.annua*-AuNPs with thiol molecule could make it a good potential drug delivery agent. The coating of *A.annua*-AuNPs with polyvinylpyrrolidone (PVP) could increase its antimicrobial activity so to improve the good stability and high antimicrobial property, the coating of the synthesized AuNPs will be done.

### 4.3. Future work

- Include the preliminary phytochemical screening (PPS) of the *Artemisia annua* plant extract to confirm the phytochemical responsible for the synthesis of *A.annua*-AuNPs.

- Improve the antimicrobial property of *A.annua*-AuNPs by either using a coating agent or doping it with biodegradable antibacterial polymers. The purification method will be also used to remove unreacted Au (III) ions and other impurities that may affect antimicrobial activity.

- Use other locally grown *Artemisia annua* plant specie to synthesize AuNPs and compare the antimicrobial properties with the one used in this project which is obtained from Kenya. This could help to possibly determine the impact that the absence or presence of phytochemicals using PPS could have on the activity of AuNPs.

- On the success in improving the MIC assay, further testing such as MBS, and evaluation of the *A.annua*-AuNPs toxicity will be done.